



## Nitrogen uptake and transformation in a midwestern U.S. stream: A stable isotope enrichment study

STEPHEN K. HAMILTON<sup>1\*</sup>, JENNIFER L. TANK<sup>2</sup>, DAVID F. RAIKOW<sup>1</sup>, WILFRED M. WOLLHEIM<sup>3</sup>, BRUCE J. PETERSON<sup>3</sup> & JACKSON R. WEBSTER<sup>4</sup>

<sup>1</sup>*Kellogg Biological Station and Department of Zoology, Michigan State University, 3700 E. Gull Lake Dr., Hickory Corners, MI 49060, U.S.A.*; <sup>2</sup>*Department of Biological Sciences, University of Notre Dame, Notre Dame, IN 46556, U.S.A.*; <sup>3</sup>*Ecosystems Center, Marine Biological Laboratory, Woods Hole, MA 02543, U.S.A.*; <sup>4</sup>*Department of Biology, Virginia Polytechnic Institute and State University, Blacksburg, VA 24061, U.S.A.*

(\*Author for correspondence; e-mail: hamilton@kbs.msu.edu)

**Key words:** ammonium, <sup>15</sup>N, nitrification, nitrogen, stable isotopes, streams

**Abstract.** This study presents a comprehensive analysis of nitrogen (N) cycling in a second-order forested stream in southern Michigan that has moderately high concentrations of ammonium (mean, 16  $\mu\text{g N/L}$ ) and nitrate (17  $\mu\text{g N/L}$ ). A whole-stream <sup>15</sup>NH<sub>4</sub><sup>+</sup> addition was performed for 6 weeks in June and July, and the tracer <sup>15</sup>N was measured downstream in ammonium, nitrate, and detrital and living biomass. Ancillary measurements included biomass of organic matter, algae, bacteria and fungi, nutrient concentrations, hydraulic characteristics, whole-stream metabolism, and nutrient limitation assays. The results provide insights into the heterotrophic nature of woodland streams and reveal the rates at which biological processes alter nitrogen transport through stream systems.

Ammonium uptake lengths were 766–1349 m and uptake rates were 41–60  $\mu\text{g N m}^{-2} \text{min}^{-1}$ . Nitrate uptake could not be detected. Nitrification rates were estimated from the downstream increase in <sup>15</sup>N-enriched nitrate using a simulation model. The ammonium was removed by nitrification (57% of total uptake), heterotrophic bacteria and fungi associated with detritus (29%), and epilithic algae (14%). Growth of algae was likely limited by light rather than nutrients, and dissolved O<sub>2</sub> revealed that the stream metabolism was heterotrophic overall (P:R = 0.1). Incubations of detritus in darkened chambers showed that uptake of <sup>15</sup>N was mostly heterotrophic.

Microbial N in detritus and algal N in epilithon appeared to reach isotopic steady state with the dissolved ammonium, but the isotopic enrichment of the bulk detritus and epilithon did not approach that of ammonium, probably due to a large fraction of organic N in the bulk samples that was not turning over. The actively cycling fraction of total N in organic compartments was estimated from the isotopic enrichment, assuming uptake of ammonium but not nitrate, to be 23% for epilithon, 1% for fine benthic organic matter, 5% for small woody debris, and 7% for leaves. These percentages agree with independent estimates of epilithic algal biomass, which were based on carbon:chlorophyll ratios in bulk samples and in algal fractions separated by density-gradient centrifugation in colloidal silica, and of microbial N in the detritus, which were based on N released by chloroform fumigations.

## Introduction

The fluxes and transformations of nitrogen in ecosystems have long interested ecologists, particularly because of the critical role of nitrogen as a limiting nutrient for biological production, and because human activities have extensively altered the N cycle (Galloway et al. 1995; Vitousek et al. 1997; Fenn et al. 1998). Nitrogen from anthropogenic sources is readily transported by groundwater flow as nitrate and appears in groundwater discharge to streams and rivers, and surface runoff and waste effluents often enrich streams with ammonium as well as nitrate (Mueller & Helsel 1996; Caraco & Cole 1999). Regional watershed mass-balance studies indicate that most of the anthropogenic N that enters watersheds is lost somewhere in transit through the hydrologic system before reaching the oceans by riverine transport (Howarth et al. 1996; Alexander et al. 2000). Streams and their riparian wetlands are suspected to be important sinks of N along hydrologic flow paths across the landscape, removing N through both assimilative uptake of N and bacterial denitrification of nitrate, although the latter process is the most important permanent sink for N in most stream ecosystems. While removal of N from stream water may reduce the eutrophication of coastal ocean waters, accelerated rates of nitrification and denitrification enhance the emission of nitrous oxide, a potent greenhouse gas, to the atmosphere (Fenchel et al. 1998).

The objective of this study was to elucidate the N cycle in a low-gradient, midwestern U.S. stream by means of a whole-ecosystem tracer experiment using  $^{15}\text{N}$ -labelled ammonium ( $^{15}\text{NH}_4^+$ ). The  $^{15}\text{NH}_4^+$  added to the stream may be assimilated by autotrophic or heterotrophic organisms, transformed to nitrate by nitrifying bacteria, or simply conveyed downstream. Stable isotope enrichment allows measurement of ambient N fluxes without significantly altering dissolved  $\text{NH}_4^+$  concentrations. This experiment is part of an intersite comparison project known as the Lotic Intersite Nitrogen eXperiment (LINX), in which similar experiments have been performed at 9 sites in diverse biomes across North America. The stream under study here, Eagle Creek, is distinct from most of the other LINX sites in that it is larger and carries higher concentrations of  $\text{NH}_4^+$  and  $\text{NO}_3^-$ . Nutrient concentrations in Eagle Creek are not unusually high for the midwestern U.S., however, where agricultural N sources are abundant and atmospheric N deposition is high (Battaglin & Goolsby 1997; Goolsby 2000).

## Study site

Eagle Creek is a second-order tributary of the Kalamazoo River that drains glacial terrain in southwestern Michigan between the cities of Kalamazoo

and Battle Creek, entering the Kalamazoo River just above the Village of Augusta. The climate is temperate and humid, with a mean annual temperature of 9.2 °C and a mean annual precipitation of 92 cm. The stream drains a watershed that is largely covered with secondary deciduous forest and successional fields and ranges in elevation from 245–460 m.a.s.l. There is presently no agriculture and little human presence in the watershed, which lies within the Fort Custer State Recreation Area and adjacent military land. Like many streams in this region, Eagle Creek and its watershed are in the process of ecological recovery from nearly complete deforestation for agriculture during the 1800's. Upstream of the study reach, Eagle Creek flows through a small reservoir (Eagle Lake), exiting the reservoir at about 1200 m above the study reach, then passes through wetlands filled with emergent marsh vegetation. Beavers had impounded the stream water at several points in the wetland reach during the experiment.

Sampling stations in the study reach are identified by their distance downstream of the  $^{15}\text{N}$  addition point (0 m), and extend to just below a railroad bridge (461 m), which is located near the confluence with the Kalamazoo River (42°20'13" N latitude, 85°20'16" W longitude). This study reach was selected mainly because it has no significant groundwater inflows or riparian wetlands. The stream channel in the study reach averages 5 m in width and 0.2 m in depth, with a longitudinal gradient of approximately 0.25%. The stream was once channelized between the 100 and 250 m sampling sites; the existence of large trees on the spoils indicates that the channel has not been altered for the past several decades. Deciduous forest shades most of the stream channel, except between the 350 and 460 m sampling sites where the trees had been partially cleared for a railroad and power line.

The stream bottom is largely covered by coarse sand (54% of the total area in the study reach) and gravel (35%), with lesser areas of cobble (10% overall, with more cobble in the lower half of the reach). Accumulations of fine organic matter occur in depositional areas along the edges, and organic matter is intermixed with the sand in variable proportions.

The water level and discharge of Eagle Creek are relatively stable as a result of limited overland runoff in the permeable glacial soils of the watershed, as well as the impounded lake and beaver ponds upstream. A storm on 26 June 1998 (Day 10 of the  $^{15}\text{N}$  release) increased the discharge and water depth at least two-fold over baseflow. Another brief discharge peak occurred on 8 August 1998 (11 days post), caused by the removal of a beaver dam in the recreation area upstream. Channel and bottom features appeared virtually unchanged after these increases in discharge.

## Methods

The crux of the LINX experiments was a 6-week  $^{15}\text{NH}_4^+$  enrichment of the stream water, with intensive sampling during and after the addition to track the fluxes of the added  $^{15}\text{N}$  through biotic and abiotic compartments. Methods employed in this experiment were standardized across the LINX study sites. To characterize the study site and provide the context for interpreting the  $^{15}\text{N}$  fluxes, we measured a variety of ecosystem characteristics shortly before and during the experiment. The methods for characterization of the study reach are described first, followed by the methods for the  $^{15}\text{N}$  addition and associated sampling and data analysis. We collected samples from seven stations distributed throughout the study reach (116, 176, 251, 301, 351, 396, and 461 m downstream of the  $^{15}\text{N}$  addition point) as well as from a reference site about 10 m upstream of the addition point (providing information on background  $^{15}\text{N}$  levels in all compartments).

### *Hydrology and hydrochemistry*

The hydraulic characteristics of the study reach were examined during the two weeks prior to the  $^{15}\text{N}$  addition period using constant-rate injections of a conservative solute ( $\text{Br}^-$ ) in conjunction with the short-term nutrient enrichments described below. A solution of NaBr (100 or 400 g/L) was added at the 0-m station using a peristaltic pump set to a flow rate of about 60 mL/min and distributed into 5 tubes spread laterally across the channel. Discharge and transient storage (expressed as the ratio of transient storage area to channel area,  $A_s:A$ ) were estimated by simulation modeling of the dilution and dispersion of the  $\text{Br}^-$  peak (Bencala & Walters 1983; Webster & Ehrman 1996; Hart 1995). Bromide additions for discharge measurement were also performed weekly throughout the experiment; daily discharge was estimated from the observed stage-discharge relationship.

Water samples for chemical analysis were filtered upon collection using Gelman Supor membranes (0.45  $\mu\text{m}$ ) and refrigerated, and concentrations of  $\text{Br}^-$  and inorganic N and P were analyzed within 1–3 days. We measured  $\text{Br}^-$  by membrane-suppressor ion chromatography. Ammonium was measured within 24 h by the indophenol blue method (Grasshoff et al. 1983; Aminot et al. 1997) using long-pathlength spectrophotometry. A correction factor for matrix interference was determined based on standard additions to filtered creek water. Nitrate was measured by membrane-suppressor ion chromatography unless it was below  $\sim 20 \mu\text{g N/L}$ , in which case we used Cd-Cu reduction followed by colorimetric analysis of nitrite (Wetzel & Likens 1991). Field measurements of dissolved  $\text{O}_2$ , pH, and conductivity were made using a YSI multisensor.

*Short-term nutrient additions and nutrient limitation assays*

Short-term enrichments of labile nutrients were used to estimate nutrient uptake lengths (i.e., the distance traveled by the nutrient in stream water before it is assimilated or transformed; Newbold et al. 1981). Orthophosphate, nitrate, and ammonium additions were performed in conjunction with  $\text{Br}^-$  additions on sequential days during the week before the  $^{15}\text{N}$  addition began, using the pump and manifold described above. Nutrient concentrations at various points along the channel downstream of the addition were measured after the  $\text{Br}^-$  concentrations had stabilized at the downstream end of the reach. These additions lasted around two hours and were designed to yield concentration increases that would be readily measurable but low enough to minimize the possibility of saturation of the biotic uptake capacity. We increased  $\text{NH}_4^+$  from 20 to 32  $\mu\text{g N/L}$ ,  $\text{NO}_3^-$  from 29 to 86  $\mu\text{g N/L}$ , and  $\text{PO}_4^{3-}$  from 2.6 to 16.8  $\mu\text{g P/L}$ .

Nutrient-diffusing substrata were deployed to investigate possible nutrient limitation of algal and fungal growth in the stream, using nutrient-amended agar (Winterbourn 1990). These experiments were repeated three times during the summer, first with glass-fiber filters or oak veneer mounted on plastic cups, then with inverted porous clay pots, and finally with Nylon membranes mounted over acrylic chambers. Treatments included controls, +N (as  $\text{NO}_3^-$ ), +P (as  $\text{PO}_4^{3-}$ ), and +N and P, and each treatment had 4–8 replicates. Algal biomass response was measured as chlorophyll-*a* fluorescence (Welshmeyer 1994) after cold extraction in 95% ethanol. Fungal biomass response on the wood veneer was measured as ergosterol (Newell et al. 1988; Tank & Webster 1998).

*Whole-stream metabolism*

Whole-stream rates of gross primary production (GPP) and community respiration (R) were determined once during the  $^{15}\text{N}$  addition period (9–10 July 1998). Dissolved  $\text{O}_2$  and temperature were monitored at 5-min intervals over the diel cycle using YSI multisensors located at two points (133 and 433 m) along the stream reach (Marzolf et al. 1994; Young & Huryn 1998). The gas exchange rate for the reach was determined from simultaneous injection of propane and a conservative solute ( $\text{Br}^-$ ). Photosynthetically-active radiation reaching the stream channel was measured around noon on a clear day (29 June 1998) at 14 cross-channel transects.

*N standing stocks in detrital and living organic matter*

During the two weeks prior to the start of the  $^{15}\text{N}$  addition, we estimated the biomass and N content of the various detrital compartments and living organisms involved in N uptake and cycling. Ash-free dry mass (AFDM) was determined by combustion of subsamples at 500 °C for four hours. Carbon and nitrogen content were measured using a Carlo Erba Model 1500 Elemental Analyzer. For fine benthic organic matter (FBOM; particles < 1 mm), AFDM and C and N content were determined after exposure to an acidic atmosphere to remove inorganic carbonates (Hedges & Stern 1984).

Standing stocks of organic matter were sampled by a stratified random approach to yield area-weighted mean densities for the entire study reach. Suspended particulate organic matter (SPOM) was collected by filtering several liters of stream water through tared glass-fiber filters (Gelman AE;  $N = 6$ ). Abundance of SPOM per unit area was calculated from concentration and the mean depth of the stream. FBOM was sampled twice, once during 1998 and again the following summer using cores (18 cm<sup>2</sup> area and 5 cm depth;  $N = 30$ ); the 1999 data are presented here because the FBOM was partitioned into upper and lower layers in that sampling. FBOM in the uppermost cm of sediment was withdrawn from each core by suction and analyzed separately. Small woody debris (> 1 mm and < 10 cm in length) and leaves were sampled from a total of sixty 730-cm<sup>2</sup> quadrats. All wood and leaves were removed by hand to a sediment depth of about 10 cm. Most leaves and wood in the stream at that time were already fragmented and partially decomposed.

Epilithon was collected from several rocks in each of 10 distinct cobble areas throughout the study reach. Material was scrubbed from a known area of rock surface using a wire brush, rinsed into plastic cups, and the resultant slurries were filtered onto glass-fiber filters (Gelman AE) for measurement of AFDM, N, and chlorophyll-a. The measured C:N ratio for epilithon could be affected by inorganic carbonates because samples were not exposed to acid prior to analysis.

Benthic invertebrates were collected using a Surber sampler (0.1 m<sup>2</sup>) at 35 points across the study reach. Invertebrates were also collected from coarse woody debris, hand-picking the organisms from known areas of wood surfaces. Unionid bivalves (Raikow & Hamilton 2001) and crayfish were sampled by collection of all individuals within several square meters of stream bottom at several points across the reach. Fishes were sampled on 26 July 1998 by electrofishing between block seines in three 50-m sections.

### *Microbial biomass and N*

Subsamples of the detrital organic matter (FBOM, small woody debris, and leaves) were collected in conjunction with the biomass measurements described above for analysis of ergosterol (as an indicator of fungal biomass) and bacterial cell counts. Samples of 5–15 g wet mass were preserved in HPLC-grade methanol (for extraction of ergosterol) or 5% buffered formalin (for bacterial abundance). Ergosterol was extracted in methanol at 80 °C for 2 hr then saponified, separated in pentane and quantified by High-Performance Liquid Chromatography (Newell et al. 1988). Bacterial cell abundance was estimated from acridine orange direct counts following homogenization and sonification to release and disperse the cells. One filter was prepared from each of the five subsamples and cells were counted for at least 5 different locations on each filter.

The N content of microbial biomass associated with detritus was measured using the chloroform fumigation technique (Brookes et al. 1985a, b). Partially decomposed wood fragments, leaves, and surface FBOM were collected from three locations in the study reach (–10 m, 301, and 400 m) on Days 14 and 35 of the  $^{15}\text{N}$  addition. Samples were kept moist during transport to the lab, where they were placed in flasks in a desiccator and exposed to chloroform in the dark at room temperature for 24 hours. Replicate subsamples were placed in a desiccator without chloroform to serve as non-fumigated controls. The fumigated and non-fumigated samples were then extracted in 0.5 M  $\text{K}_2\text{SO}_4$ , and the extracts were filtered and frozen until analysis. Total N was determined by alkaline persulfate digestion of the extracts (Cabrera & Beare 1993), followed by Cd-Cu reduction of nitrate and colorimetric analysis of the resultant nitrite. Mass of microbial N was calculated as the difference in total N between fumigated and non-fumigated  $\text{K}_2\text{SO}_4$  extracts, divided by 0.54 (Brookes et al. 1985b) to account for incomplete extraction of microbial biomass N over 24 hours. Microbial N mass was then normalized to AFDM using wet mass-AFDM conversions determined for each sample type. Microbial N as a fraction of total N for each material type was calculated using the AFDM-normalized microbial N values and values of total N content per unit AFDM determined from the C:N ratio and dry mass/AFDM conversions.

### *Addition of the $^{15}\text{N}$ tracer*

The  $^{15}\text{N}$  tracer addition was designed to produce a readily measurable enrichment in the  $\delta^{15}\text{N}$  of the dissolved  $\text{NH}_4^+$  (i.e., to ca. 500‰), based on the stream discharge and  $\text{NH}_4^+$  concentration at the start of the addition period. A peristaltic pump continuously dripped a solution of  $^{15}\text{N}$ -enriched  $\text{NH}_4\text{Cl}$  (10 atom%  $^{15}\text{N}$ ) into the stream at 2 mL/min to achieve the target rate of 506 mg

$^{15}\text{N}/\text{d}$ . Several wooden planks were staked in place in the channel just below the dripper to enhance cross-channel mixing. The addition began on 16 June 1998 (Day 0) and terminated on 28 July (Day 42). Throughout the addition, the pump flow rate was monitored daily and readjusted if necessary.

#### *Measurement of $\delta^{15}\text{N}$ in dissolved N*

Water samples for analysis of  $\delta^{15}\text{N}$  in  $\text{NH}_4^+$  ( $\delta^{15}\text{N-NH}_4^+$ ) and  $\text{NO}_3^-$  ( $\delta^{15}\text{N-NO}_3^-$ ) were collected on days 0 (approximately six hours after initiating the  $^{15}\text{N}$  addition), 20, and 41 during the addition, and 13–17.5 hours after the end of the addition (day 1 post). Short-term  $\text{Br}^-$  additions were performed to determine discharge each time that water samples were collected for  $\delta^{15}\text{N}$ . Two 4-L samples of stream water were collected from each station with a peristaltic pump, filtering the water through a glass fiber filter (Whatman GF/F). Additional samples for  $\delta^{15}\text{N-NO}_3^-$  were taken from stations at 201 and 426 m. We sampled water at the same time for analysis of  $\text{NH}_4^+$  and  $\text{NO}_3^-$  concentrations.

The  $\delta^{15}\text{N-NH}_4^+$  was measured in one of the two 4-L samples taken at each station using the ammonia diffusion procedure of Holmes et al. (1998), in which  $\text{MgO}$  is added to elevate the pH and the  $\text{NH}_3$  diffuses into an acidified glass-fiber filter sealed within a Teflon packet floating on the surface of the sample. The second 4-L sample from each station was analyzed for  $\delta^{15}\text{N-NO}_3^-$  using the method of Sigman et al. (1997), in which  $\text{NH}_4^+$  is removed from the sample by adding  $\text{MgO}$  and boiling, then DeVarda's Alloy is added to reduce  $\text{NO}_3^-$  to  $\text{NH}_3$  so it could be absorbed onto a filter as described above. The  $\delta^{15}\text{N}$  of total dissolved N was measured in a few samples from day 1 post by UV oxidation, followed by collection of the resultant inorganic N as described above. The  $\delta^{15}\text{N-DON}$  was estimated by correcting for the contributions of  $\text{NH}_4^+$  and  $\text{NO}_3^-$  to the  $\delta^{15}\text{N}$  of the total dissolved N.

#### *Sample collection for $\delta^{15}\text{N}$ in organic matter*

Detrital organic matter and living organisms were sampled weekly for  $\delta^{15}\text{N}$  during the  $^{15}\text{N}$  tracer addition and for 1 month after the addition was completed. At each station, we generally collected composite samples from multiple locations. For invertebrates, multiple individuals were combined to make a sample, and live organisms were placed in water overnight to allow their gut contents to clear before they were dried and ground. Whole-body samples were analyzed for  $\delta^{15}\text{N}$  except for unionid bivalves and adult crayfish, from which we dissected muscle tissue. Fish were collected on Day 40 for  $\delta^{15}\text{N}$  analysis of muscle tissue. Detrital organic matter and organisms were



dried at 50 °C and ground to a fine powder before subsampling for isotopic analysis.

#### *$\delta^{15}\text{N}$ in the algal fraction of epilithon*

Samples of biofilms on rocks (epilithon) were collected on 18 July 1998 (Day 32) for separation of the algal fraction, following the methods of Hamilton and Lewis (1992). The purpose of this sampling was to determine how well our measurements of the  $\delta^{15}\text{N}$  in bulk epilithon corresponded with the  $\delta^{15}\text{N}$  of the algal fraction of that material. Epilithon was scrubbed from rocks collected around 351 and 461 m, immediately placed on ice in a dark cooler, and processed within 24 hours. Slurries of the material scrubbed from surfaces were first subsampled and collected on GF/F filters as in the regular protocol ('bulk samples'). Another subsample of the slurry was centrifuged in water, leaving some algae in the supernatant. The resultant pellet was subsequently disaggregated and centrifuged over colloidal silica (Ludox AM-30 from DuPont; specific gravity = 1.21), yielding an algae-rich upper layer and a detritus-rich lower layer. The material in the upper layer was combined with the algae collected from the supernatant to make the 'algal fraction', while the pellet at the bottom of the tube was collected as the 'detrital fraction'.

The algal and detrital fractions were collected on quartz-fiber filters (Whatman QM/A), which were immediately frozen and later subsampled using a paper punch. We evaluated the efficacy of the separations by measuring the C, N and chlorophyll-*a* content in the two separated fractions, using the analytical methods already described. Subsamples were exposed to an acidic atmosphere to remove inorganic carbonates (Hedges & Stern 1984) prior to measurement of organic carbon content with the Elemental Analyzer. The C and chlorophyll contents in the original slurry were estimated by summation of the C and chlorophyll contents of the two separated fractions. Algae in the subsamples were enumerated by R. Dufford.

#### *In-situ incubations of detrital organic matter*

To determine rates of microbial colonization and subsequent  $^{15}\text{N}$  uptake, leaves and wood were incubated at a single station (396 m) and periodically sampled for isotopic analysis during and shortly after the  $^{15}\text{N}$  tracer addition. Senescent leaves were collected in March from branches of American Beech (*Fagus grandifolia*), White Oak (*Quercus alba*), and Black Oak (*Quercus velutina*). The leaves were dried at 50 °C and mounted with Nylon line as replicated leaf packs arranged randomly along the sides of fiberglass rain

gutters. In addition, oak dowel segments were mounted in the centers of the gutters.

The gutters containing detrital samples were installed in the stream eight weeks prior to the start of the  $^{15}\text{N}$  addition to allow time for microbial colonization. The gutters were located at 396 m and oriented parallel to the direction of flow, with the samples in the middle of the water column. To examine the effect of light on the detrital  $\delta^{15}\text{N}$ , half of the gutters were covered with an opaque, black acrylic sheet and the remaining half were covered with a clear acrylic sheet. The sheets were periodically cleaned throughout the incubation period.

Samples were collected on the day prior to start of the addition, days 7, 21, 34, and 41 during the addition, and 8 days after the addition ended. Leaves were removed from the surface of each leaf pack and combined to make a composite sample from each treatment (light and dark). For the wood dowel, we removed each segment and scraped off the soft outer layer, collecting composite samples of the particulate material on glass-fiber filters. Invertebrates were removed from the detritus by hand. In addition to measurements of  $\delta^{15}\text{N}$ , subsamples were analyzed for chlorophyll-*a* as an indicator of attached algal biomass and ergosterol as an indicator of fungal biomass, using the methods described earlier.

#### *Stable isotope measurements*

Stable N isotope analyses were performed at the Ecosystems Center, Marine Biological Laboratory, Woods Hole, Massachusetts, or the Center for Environmental Science and Technology at the University of Notre Dame, South Bend, Indiana. Both laboratories used automated analytical systems in which the isotope ratio mass spectrometer was coupled to a high temperature combustion column and cryogenic separation unit. Samples analyzed at both labs showed good agreement. Stable isotope measurements are expressed as  $\delta^{15}\text{N}$  (units of ‰) according to the following equation:

$$\delta^{15}\text{N} = [(R_{\text{sample}}/R_{\text{standard}}) - 1] \times 1000 \quad (1)$$

where  $R = ^{15}\text{N}:^{14}\text{N}$  ratio, and the  $^{15}\text{N}$  isotope standard is air ( $R_{\text{standard}} = 0.0036765$ ). All  $\delta^{15}\text{N}$  values and  $^{15}\text{N}:^{14}\text{N}$  ratios reported in this study reflect tracer  $^{15}\text{N}$  only because background  $\delta^{15}\text{N}$  measurements made at the upstream reference site were always subtracted from  $\delta^{15}\text{N}$  measurements made in the enriched reach (Peterson et al. 1997).

The mass of tracer  $^{15}\text{N}$  in each organic (biomass) compartment ( $^{15}\text{N}_{\text{biomass}}$ ,  $\text{mg}/\text{m}^2$ ) was determined from the background-corrected  $\delta^{15}\text{N}$  ( $\delta^{15}\text{N}_{\text{biomass}}$ )

and the total N standing stock ( $TN_{\text{biomass}}$ , as measured just prior to the  $^{15}\text{N}$  addition) as follows:

$$^{15}\text{N}_{\text{biomass}} = (\delta^{15}\text{N}_{\text{biomass}}/1000) \times 0.003663 \times TN_{\text{biomass}} \quad (2)$$

#### *Ammonium uptake length and rate*

The uptake length for  $^{15}\text{NH}_4^+$  was calculated as the inverse of the slope of the regression of the natural logarithm of tracer  $^{15}\text{NH}_4^+$  flux on distance, which is analogous to the uptake length calculation for short-term nutrient additions (Newbold et al. 1981). Uptake lengths were calculated on the three dates when  $\delta^{15}\text{N-NH}_4^+$  was measured (days 0, 20, and 41). The  $^{15}\text{NH}_4^+$  fluxes across the study reach would overestimate  $\text{NH}_4^+$  uptake length if there was significant regeneration of tracer  $^{15}\text{NH}_4^+$  from biomass compartments back to the stream water, and such regeneration would become more important over the course of the  $^{15}\text{N}$  addition as the tracer  $^{15}\text{N}$  accumulated in biomass. The tracer  $\delta^{15}\text{N-NH}_4^+$  measurements for each station on day 1 post reflect the maximum rate of regeneration of  $^{15}\text{NH}_4^+$  from biomass back to water. As an approximate correction for  $^{15}\text{NH}_4^+$  regeneration, we subtracted 50% of the tracer  $\delta^{15}\text{N-NH}_4^+$  measured on day 1 post from the tracer  $\delta^{15}\text{N-NH}_4^+$  measurements on day 20, and the entire post-addition  $\delta^{15}\text{N-NH}_4^+$  from the  $\delta^{15}\text{N-NH}_4^+$  measurements on day 41 (Mulholland et al. 2000). However, these regeneration corrections reduced the estimated uptake lengths by only ca. 10%.

Whole-stream ammonium uptake rates ( $\text{mg N m}^{-2} \text{d}^{-1}$ ) were computed by dividing the average reach flux of  $\text{NH}_4^+$  in stream water (discharge  $\times$   $\text{NH}_4\text{-N}$  concentration) by the product of the ammonium uptake length (as estimated from  $\delta^{15}\text{N-NH}_4^+$  above) and the average top width of the stream (5 m) (Newbold et al. 1981). Rates of ammonium uptake by specific biomass compartments were calculated from the tracer  $^{15}\text{N}$  in the biomass compartments on Day 7 for individual sampling stations ( $^{15}\text{N}_{\text{biomass, day 7}}$ ) and the mean tracer  $^{15}\text{N}:^{14}\text{N}$  ratios in dissolved  $\text{NH}_4^+$  at those stations ( $^{15}\text{N}_{\text{water ratio, days 0-7}}$ ) as follows:

$$\text{Compartment } \text{NH}_4^+ \text{ uptake rate} = \quad (3)$$

$$(^{15}\text{N}_{\text{biomass, day 7}})(^{15}\text{N}_{\text{water ratio, days 0-7}})^{-1}(7\text{d})^{-1}$$

where  $^{15}\text{N}_{\text{biomass, day 7}}$  was calculated from equation 2 and  $^{15}\text{N}_{\text{water ratio, days 0-7}}$  was calculated as  $(\delta^{15}\text{N-NH}_4/1000) \times 0.003663$ , using the mean of the calculated  $\delta^{15}\text{N-NH}_4^+$  values for Days 0–7. Compartments with rapid N turnover would have lost some tracer  $^{15}\text{N}$  by day 7, which would result in an underestimation of  $^{15}\text{N}$  uptake rates. To account for turnover, the values

of  $^{15}\text{N}_{\text{biomass, day 7}}$  were multiplied by correction factors determined from the measured turnover rates of  $^{15}\text{N}$  in each compartment. Turnover rates were estimated from the observed decline in  $\delta^{15}\text{N}$  over the first 28 days following termination of the  $^{15}\text{N}$  addition, using the tracer accumulation model described by Mulholland et al. (2000). The  $^{15}\text{N}$  turnover correction factors ranged from 1.21 for wood (with the lowest  $^{15}\text{N}$  turnover rate) to 1.97 for leaves (with the highest  $^{15}\text{N}$  turnover rate).

#### *Nitrification rate and nitrate uptake rate and length*

Nitrification rate and nitrate uptake rate were determined by fitting a two-compartment (streamwater  $^{15}\text{NH}_4^+$  and  $^{15}\text{NO}_3^-$ ) mass-balance model to the longitudinal profile for  $^{15}\text{NO}_3^-$  flux ( $\mu\text{g } ^{15}\text{N/s}$ ) determined from the measured values of  $\delta^{15}\text{N}\text{-NO}_3^-$ , nitrate concentration, and stream discharge. The model describes the change in  $^{15}\text{NH}_4^+$  (A) and  $^{15}\text{NO}_3^-$  (N) flux over distance  $x$  (Figure 1(a)) and is described in more detail by Mulholland et al. (2000). The model equations are:

$$\partial A/\partial x = -k_1 A \quad (4)$$

$$\partial N/\partial x = k_N A - k_2 N \quad (5)$$

where  $k_1$  (equal to  $k_B + k_N$  in Figure 1(a)) is the measured rate of decline in streamwater  $^{15}\text{NH}_4^+$  with distance due to both assimilative uptake and nitrification (equivalent to the inverse of uptake length, uncorrected for  $^{15}\text{NH}_4^+$  regeneration, in units of  $\text{m}^{-1}$ ),  $k_N$  is the nitrification rate per unit distance [in units of  $\mu\text{g } \text{NO}_3^- \text{-N} (\mu\text{g } \text{NH}_4^+ \text{-N})^{-1} \text{m}^{-1}$ , or  $\text{m}^{-1}$ ], and  $k_2$  is the  $^{15}\text{NO}_3^-$  uptake rate per unit distance [in units of  $\mu\text{g } \text{NO}_3^- \text{-N} (\mu\text{g } \text{NO}_3^- \text{-N})^{-1} \text{m}^{-1}$ , or  $\text{m}^{-1}$ ]. The solution to equation 4 is:

$$A = A_0 e^{-k_1 x} \quad (6)$$

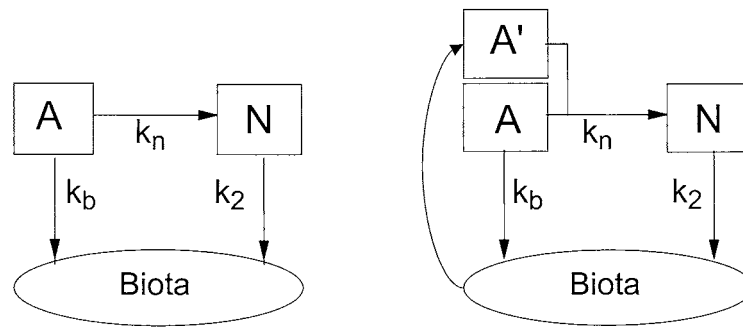
where  $A_0$  is the flux of  $^{15}\text{NH}_4^+$  (units of  $\mu\text{g } ^{15}\text{N/s}$ ) at  $x = 0$  m. We used the 176-m station as the starting point ( $x = 0$ ) for the modeling because this was the uppermost station at which the added tracer was thoroughly mixed across the channel.

Substituting for A (from equation 6) into equation 5, the solution for N (units of  $\mu\text{g } ^{15}\text{N/s}$ ) is:

$$N = [(k_N A_0)/(k_2 - k_1)](e^{-k_1 x} - e^{-k_2 x}) + N_0 e^{-k_2 x} \quad (7)$$

where  $N_0$  is the  $^{15}\text{NO}_3^-$  flux at the 176-m station. We applied a least-squares fitting procedure to determine the values of  $k_N$  and  $N_0$  that best fit

(a) Nitrification, Day 0      (b) Nitrification, Days 20, 41



(c) Regeneration of N,  
Day 1 post

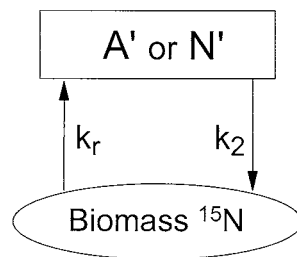


Figure 1. Schematic depiction of simulation models used to estimate rates of N assimilation, nitrification, and N regeneration. (a) nitrification on day 0, where  $A = {}^{15}\text{NH}_4^+$  flux ( $\mu\text{g } {}^{15}\text{N/s}$ ) at the addition point,  $N = {}^{15}\text{NO}_3^-$  flux,  $k_B = \text{NH}_4^+$  uptake rate,  $k_N =$  nitrification rate, and  $k_2 = \text{NO}_3^-$  uptake rate; (b) nitrification on days 20 and 41, where  $A$ ,  $N$ , and the rates are the same as in 1A except that the  ${}^{15}\text{NH}_4^+$  flux is partitioned into  ${}^{15}\text{N}$  from the dripper ( $A$ ) and  ${}^{15}\text{N}$  regenerated from biomass compartments ( $A'$ ); (c) regeneration of  $\text{NH}_4^+$  or  $\text{NO}_3^-$  on day 1 post, where  $\text{Biomass } {}^{15}\text{N}$  has units of  $\mu\text{g } {}^{15}\text{N/m}$  stream length,  $A'$  or  $N'$  represent regenerated  ${}^{15}\text{NH}_4^+$  or  ${}^{15}\text{NO}_3^-$ ,  $k_r$  is the rate of  ${}^{15}\text{NH}_4^+$  or  ${}^{15}\text{NO}_3^-$  regeneration from biomass (units of  $\text{s}^{-1}$ ), and  $k_2$  is the uptake rate of regenerated  ${}^{15}\text{NH}_4^+$  or  ${}^{15}\text{NO}_3^-$  (in units of  $\text{m}^{-1}$ ).

the observed longitudinal tracer  ${}^{15}\text{NO}_3^-$  flux distributions, assuming that  $k_2$ , which determines the rate of the  ${}^{15}\text{NO}_3^-$  decline downstream, was zero since we could not detect  $\text{NO}_3^-$  uptake across the reach.  $N_0$  was fitted to avoid reliance on a single measured value of  $\delta^{15}\text{N}-\text{NO}_3^-$ . For day 0,  $A_0$  is the  ${}^{15}\text{NH}_4^+$  advective flux at  $x = 0$ , determined from the addition rate and the longitudinal

profile of  $\delta^{15}\text{N-NH}_4$ . As we did in calculating  $\text{NH}_4^+$  uptake, we applied a small correction for  $^{15}\text{NO}_3^-$  regeneration by subtracting the entire  $^{15}\text{NO}_3^-$  flux observed on day 1 post from the day 40 estimate, and half of that flux from the day 20 estimate.

#### *Nitrogen regeneration and turnover rates*

The rate of regeneration of tracer  $^{15}\text{NH}_4^+$  from biomass to the stream water was determined on day 1 post using a different version of the two-compartment model (Figure 1(c)). For this application, biomass  $^{15}\text{N}$  is the sum of the  $^{15}\text{N}$  in biomass compartments potentially contributing to regeneration in units of  $\mu\text{g } ^{15}\text{N}/\text{m}$  stream length,  $A'$  or  $N'$  is streamwater  $^{15}\text{NH}_4^+$  or  $^{15}\text{NO}_3^-$  advective flux,  $k_r$  is the rate of  $^{15}\text{N}$  regeneration from biomass (units of  $\text{s}^{-1}$ ), and  $k_2$  is the uptake rate of regenerated  $^{15}\text{N}$  (in units of  $\text{m}^{-1}$ ). The longitudinal rate of decline ( $k_1$ ) of the source of  $^{15}\text{N}$  regenerated to water was assumed to be the decline in the sum of total biomass  $^{15}\text{N}$  per unit area (epilithon, FBOM, wood, and leaves) measured on day 42.  $A_0$  was determined by extrapolating the biomass  $^{15}\text{N}$  upstream to the addition point. The model was then fit to the day 1 post longitudinal flux profiles to determine  $k_r$  and  $k_2$ , as described for the nitrification application.

Turnover rates of tracer  $^{15}\text{N}$  in specific biomass compartments were determined from the decline in biomass  $\delta^{15}\text{N}$  at the 116-m station over the first 28 days after termination of the  $^{15}\text{N}$  addition, assuming first-order dynamics [i.e., from the slope of the relationship between  $\ln(\delta^{15}\text{N}_{\text{biomass}})$  and time]. Turnover rates in the incubation experiment were determined from the decline between day 41 and day 7 post, since no samples were collected after that time. These turnover estimates assume no re-uptake of the  $^{15}\text{N}$  released to the water, and thus may result in slight underestimates of turnover rate. Turnover times were calculated as the inverse of turnover rate.

#### *Total $^{15}\text{N}$ retention and export*

The total quantity of tracer  $^{15}\text{N}$  retained throughout the 461-m study reach by the end of the addition period (day 42) was estimated for each compartment by integration of the exponential rate of decline in tracer  $^{15}\text{N}$  with distance downstream, assuming a stream width of 5 m. If the slope as determined by linear regression of  $\ln(^{15}\text{N}_{\text{biomass}})$  on distance was not significant at  $P = 0.05$ , then we used the mean  $^{15}\text{N}_{\text{biomass}}$  for the study reach.

The rates of export of tracer  $^{15}\text{N}$  out of the study reach as  $\text{NH}_4^+$ ,  $\text{NO}_3^-$ , DON, and SPOM were determined from the stream discharge ( $Q$ ) and the mean concentration  $[\text{N}]$  and tracer  $\delta^{15}\text{N}$  of each form of N:

$$^{15}\text{N export rate} = (\delta^{15}\text{N}/1000) * 0.003663 * Q * [\text{N}] \quad (8)$$

Total export of tracer  $^{15}\text{N}$  in stream water over the 42-day addition period was computed by interpolation between measurement dates and integrating the daily fluxes over time. The  $\delta^{15}\text{N}$ -DON was estimated only at the end of the experiment (day 1 post), so we assumed that the observed enrichment at that time represented day 42 as well, and that the enrichment increased linearly from zero over the course of the 42-day addition period.

## Results

### *Hydrology and hydrochemistry*

The discharge of Eagle Creek was stable during most of the  $^{15}\text{N}$  addition, with a median of 199 L/s over the 42-day period (Figure 2(a)). The  $\text{Br}^-$  additions showed no detectable dilution, indicating that lateral inputs of groundwater along the study reach were small (i.e., < 5% of the discharge). The simulation modeling of the dilution and dispersion of the  $\text{Br}^-$  peak during additions in June yielded the following estimates of the hydraulic features of the channel in the study reach: Discharge 263 L/s; mean depth 18 cm; mean velocity 24 cm/s, relative transient storage zone size ( $A_s:A$ ) of 0.25, and an exchange coefficient ( $\alpha$ ) between the transient storage zones and the stream water of  $0.002 \text{ s}^{-1}$ . Discharge was lower during the  $^{15}\text{N}$  addition, but there was little change in channel width and depth. The  $\text{Br}^-$  additions also showed that when a conservative tracer is added at a single point at 0 m (as was done for  $^{15}\text{N}$ ), there was incomplete mixing at the uppermost sampling site (116 m), but mixing was complete by the following station (176 m).

Concentrations of both  $\text{NH}_4^+$  and  $\text{NO}_3^-$  decreased considerably over the course of the addition but remained similar to each other (Figure 2(b)). Nutrient concentrations measured over the course of the  $^{15}\text{N}$  addition yielded the following means (ranges in parentheses):  $\text{NH}_4^+$ -N 16  $\mu\text{g/L}$  (8–23),  $\text{NO}_3^-$ -N 17  $\mu\text{g/L}$  (7–32), total dissolved N 260  $\mu\text{g/L}$  (190–328), SRP 3.1  $\mu\text{g/L}$  (1.8–5.6), and total dissolved P 7.6  $\mu\text{g/L}$  (3–14). Eagle Creek carries water that is rich in dissolved calcium, magnesium and bicarbonate; several samples collected during the summer of 1998 showed the following means: conductivity 337  $\mu\text{S/cm}$ , pH 7.54, and total alkalinity 3.01 meq/L.

Monthly sampling of the stream between February and June 1998 as well as a single sampling in October 1998 showed similar major solute and nutrient concentrations, with dissolved oxygen saturation ranging from 64–94%. A longitudinal survey of hydrochemistry on 20 August 1998 indicated that the wetlands between the lake outflow and the upper end of the study reach were the likely source of most of the streamwater  $\text{NH}_4^+$ . Concentrations of  $\text{NH}_4^+$ -N increased from 9 to 60  $\mu\text{g/L}$  between the lake outflow and the

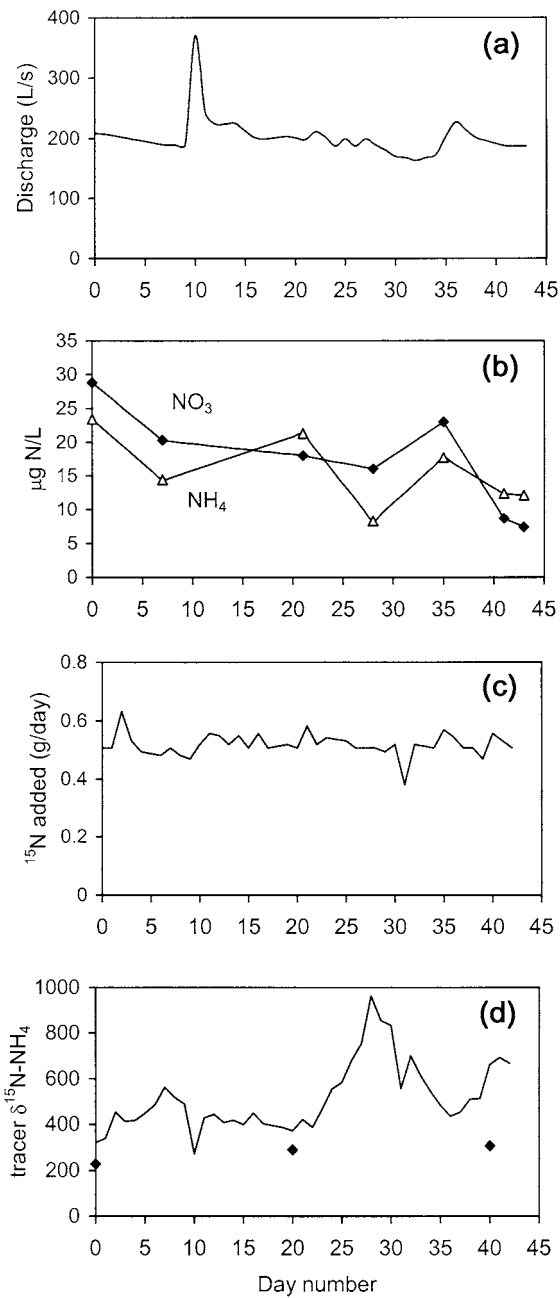


Figure 2. Stream discharge (a), mean concentrations of  $\text{NH}_4^+$  and  $\text{NO}_3^-$  for 8 stations across the study reach (b), rate of addition of  $^{15}\text{N}$  (c), and the resultant enrichment in  $\delta^{15}\text{N-NH}_4^+$  at the addition point (d) over the course of the 42-day experiment. The lower panel includes both the directly measured values of  $\delta^{15}\text{N-NH}_4^+$  (diamonds) as well as values calculated from the  $^{15}\text{N}$  addition rate and stream discharge (line); the latter are considered more accurate (see text and Table 3 for explanation).



beaver pond outflow, then fell to 42  $\mu\text{g/L}$  by the upper end of the study reach and 37  $\mu\text{g/L}$  by the lower end. Concentrations of  $\text{NO}_3^-$  were undetectable by ion chromatography (i.e.,  $< 15 \mu\text{g N/L}$ ) at the lake and beaver pond outflows, then rose to 17  $\mu\text{g N/L}$  at 0 m and 35  $\mu\text{g N/L}$  at the lower end.

#### *Short-term nutrient additions and nutrient limitation assays*

During the short-term additions of ammonium, nitrate, or orthophosphate, we did not detect a downstream decrease in concentrations; the linear regression of the natural logarithm of the nutrient concentration (corrected for background concentration and divided by the bromide concentration) on distance downstream from the addition point did not reveal a significant slope. Thus uptake rates were too low to produce a measurable reduction in concentrations, or uptake and regeneration were in approximate balance.

The experiments with nutrient-diffusing substrata showed no detectable effect of inorganic N or P addition on algal biomass, as measured on either glass-fiber filters, membrane filters or wood veneer; chlorophyll-a on the substrates averaged  $11 \pm 3 \text{ mg/m}^2$  (all treatments and experiments pooled; mean  $\pm$  s.d.,  $N = 59$ ). Fungal biomass on the wood veneer, as indicated by ergosterol content, did respond positively to both the P and N+P treatments (J.L. Tank, unpublished data). The molar ratios of dissolved inorganic N to SRP in the stream water averaged 23.5, suggesting P would be the most likely limiting nutrient.

#### *Whole-stream metabolism*

Dissolved  $\text{O}_2$  in Eagle Creek was consistently undersaturated with respect to atmospheric equilibrium, indicating that heterotrophic metabolism exceeded photosynthesis in the stream. The diel metabolism study, which was conducted during a period of clear skies, showed net heterotrophy despite the relatively high irradiance. At the downstream site (426 m), the diel variation in dissolved  $\text{O}_2$  saturation and temperature on 9–10 July ranged from 80–92% and 23–26  $^\circ\text{C}$ , respectively. The  $\text{O}_2$  reaeration rate coefficient for the study reach was 0.021/min at 25  $^\circ\text{C}$ . The gross primary production (GPP) for this period was  $0.8 \text{ g O}_2 \text{ m}^{-2} \text{ d}^{-1}$  and the community respiration (R) was  $6.4 \text{ g O}_2 \text{ m}^{-2} \text{ d}^{-1}$ , yielding a GPP:R of 0.1. Light reaching the stream channel, measured using a PAR sensor, averaged 28% of full sunlight across the entire study reach, but was higher (47%) in the lowermost section (325–426 m).

Table 1. Biomass (as AFDM, g/m<sup>2</sup>), mass ratios of C:chlorophyll-*a* (C:Chl) and C:N, and N standing stock (g/m<sup>2</sup>) of the primary uptake compartments (algae and detritus) and animals that were sampled in the study

Compartment	AFDM	C:Chl	C:N	N stock
Epilithon	5.84	165	13.9	0.31
FBOM (upper cm)	164	841	14.1 <sup>a</sup>	6.1
FBOM (upper 5 cm)	922	—	14.3 <sup>a</sup>	33.4
Small woody debris (< 2 cm)	198	—	36.6	2.6
Leaves	0.90	—	18.2	0.030
SPOM	0.59	571	~ 14 <sup>b</sup>	0.023
Sum of above	1127			36.4
Benthic insects + amphipods	0.34	—	3.6–6.3	0.0343
Unionid bivalves	1.93	—	4.1	0.196
Crayfish	0.55	—	4.4	0.063
Fishes	0.83	—	4.1	0.074
Sum of consumers	3.65			0.368

<sup>a</sup>Measured in July 1999.

<sup>b</sup>Not measured; assumed similar to FBOM.

### Biomass and N standing stocks

Reach-weighted mean densities for biomass (as AFDM) and N, as well as C:Chl and C:N mass ratios, are presented in Table 1 for the primary uptake compartments and consumers in the study reach. At the time of the experiment, the largest N pool was detrital organic matter that occurred as FBOM and small woody debris. Only the upper cm of the FBOM deposits was sampled for  $\delta^{15}\text{N}$  in this study, so the densities for that layer are used in all calculations. Freshly fallen leaves were scarce in the stream compared with other times of the year since most inputs from the deciduous trees occur in the fall (October–November). Epilithon comprised a relatively small pool of N and the reach-weighted mean chlorophyll-*a* density in epilithon was 7.2 mg/m<sup>2</sup>. Animal biomass comprised about 1% of the total N standing stock in the stream, and several species of unionid bivalves accounted for more than half of the total animal biomass and N (Raikow & Hamilton 2001).

#### *Microbial biomass and N*

Microbial biomass, as estimated from bacterial cell counts and fungal ergosterol measurements, was dominated by bacteria in FBOM, while fungi dominated in woody debris and leaves (Table 2). The sum of bacterial and fungal biomass comprised < 1% of the total organic matter in the bulk detrital

*Table 2.* Microbial biomass and N in detritus. Bacterial biomass was estimated from cell counts in samples collected just prior to the experiment, assuming a conversion factor of 0.02 pg C/cell. Fungal biomass was estimated from ergosterol concentration measured in samples collected just prior to the experiment, assuming a conversion factor of 1 mg C/11  $\mu$ g ergosterol. Microbial N was measured by the chloroform fumigation procedure; values are means (s.d.) for six replicates, and the results for days 14 and 35 are statistically indistinguishable at  $P = 0.05$

Detrital Compartment	Bacterial biomass (mg C/m <sup>2</sup> )	Fungal biomass (mg C/m <sup>2</sup> )	Microbial N (% of total N)	
			Day 14	Day 36
FBOM	174	19	1.24 (0.54)	1.21 (0.33)
Small woody debris	39	180	2.63 (0.77)	4.63 (0.97)
Leaves	0.5	3.4	8.23 (3.12)	8.03 (1.54)

compartments. Nitrogen in microbial biomass was estimated by chloroform fumigation and compared to the total N in each compartment (Table 2). Microbial nitrogen comprised the smallest fraction of total N in FBOM (1.2%), and was relatively more abundant in small woody debris (3.6%) and leaves (8.1%), with no significant difference between samples taken on Days 14 and 36 (Table 2).

#### *Isotopic enrichment of dissolved N in the stream*

The  $\delta^{15}\text{N-NH}_4^+$  in the stream water during the  $^{15}\text{N}$  addition was calculated from the  $\text{NH}_4^+$  concentrations measured by colorimetry, daily discharge estimates, and the  $^{15}\text{N}$  addition rate (as estimated from daily measurements of the rate at which the  $^{15}\text{N}$  solution was dripped into the stream) (Figure 2(d)). The large peak around Day 28 resulted from the combination of low discharge and low  $\text{NH}_4^+$  concentrations, resulting in less dilution of the added  $^{15}\text{NH}_4$ . Over the 42-day addition, the calculated  $\delta^{15}\text{N-NH}_4^+$  averaged 515‰ (background-corrected) at the addition point; background values of  $\delta^{15}\text{N-NH}_4^+$  averaged 6.8‰.

The calculated  $\delta^{15}\text{N-NH}_4^+$  can be compared with our direct measurements made on three dates. The calculation of  $\delta^{15}\text{N-NH}_4^+$  assumes complete and conservative mixing of the added  $^{15}\text{N}$  in the stream water (i.e., no uptake or regeneration of  $\text{NH}_4^+$ ), and is therefore valid only for immediately downstream of the addition point. We estimated the  $\delta^{15}\text{N-NH}_4^+$  at the addition point by linear regression of the natural logarithm of measured  $\delta^{15}\text{N-NH}_4^+$  on distance, excluding the 116-m station when it appeared to be an outlier because we know from the  $\text{Br}^-$  additions that the tracer at this site is sometimes not completely mixed across the channel. The  $\delta^{15}\text{N-NH}_4^+$  values used

in this calculation were corrected for  $\text{NH}_4^+$  regeneration as described in the methods for uptake length determination.

The estimates of  $\delta^{15}\text{N-NH}_4^+$  at the addition point based on direct measurements were consistently lower than the calculated values, with the greatest difference on Day 41 (Figure 2(d)). This discrepancy suggests that the measured  $\delta^{15}\text{N-NH}_4^+$  values may be too low, which could be explained by error in the reagent blank correction or by deamination of dissolved organic N (DON) during the sample processing for  $\delta^{15}\text{N-NH}_4^+$  (Holmes et al. 1998). DON concentrations were an order of magnitude higher than  $\text{NH}_4^+$  concentrations, and the deamination of a small fraction of this N could dilute the isotopic ratio of the dissolved  $\text{NH}_4^+$ , since the  $^{15}\text{N}$  enrichment of DON was very low (see below). Alternatively, the measured  $\delta^{15}\text{N-NH}_4^+$  values could be accurate and the colorimetric measurements of  $\text{NH}_4^+$  could be biased due to interferences and other problems known to affect this analysis (Aminot et al. 1997), but we took care to avoid such problems and therefore our colorimetric measurements are unlikely to be that inaccurate. The apparent bias in  $\delta^{15}\text{N-NH}_4^+$  measurements should have affected all samples equally, and thus the longitudinal trends in the  $\delta^{15}\text{N-NH}_4^+$  measurements should reflect the dynamics of dissolved  $\text{NH}_4^+$  in the stream. The actual  $\delta^{15}\text{N-NH}_4^+$  measurements were corrected for this apparent bias, as shown in Table 3, in all subsequent calculations in which the absolute values are critical. The parameters for the N mass-balance modeling (Figure 1) were estimated from the  $^{15}\text{N}$  fluxes across the study reach, which in turn were determined from the  $\delta^{15}\text{N}$  values and N yields measured by mass spectrometry. A consistent bias caused by additional unenriched N from reagents or DON would therefore not affect the model results.

The  $\delta^{15}\text{N-NO}_3^-$  was enriched over background on the three sampling dates during the  $^{15}\text{N}$  addition, with the enrichment increasing in the downstream direction through the study reach ( $\delta^{15}\text{N}$  data not shown). The mean enrichment across the study reach ranged from 8 to 17‰ during the addition, falling to 1.6 on day 1 post. We also measured the  $\delta^{15}\text{N-DON}$  for a few samples from day 1 post, to indicate the rate of regeneration of  $\text{DO}^{15}\text{N}$  from  $^{15}\text{N}$ -enriched organic matter at the end of the addition period. Samples from 3 stations showed a mean enrichment of 2.0‰ over the reference station. This estimate of tracer  $^{15}\text{N}$  in DON is used only for the estimation of  $^{15}\text{N}$  exported from the study reach by advective transport of DON.

#### *Nitrogen uptake and transformation*

The  $\delta^{15}\text{N-NH}_4^+$  decreased downstream from the  $^{15}\text{N}$  addition point on each of the three sampling dates (Figure 3), although the decrease appeared linear rather than the exponential decline that would be expected for a labile nutrient

Table 3. Original measurements and corrected values for  $\delta^{15}\text{N-NH}_4^+$ . The  $\delta^{15}\text{N-NH}_4^+$  at the addition point (0 m) was calculated as described in the text. For the downstream stations, the corrected  $\delta^{15}\text{N-NH}_4^+$  measurements were determined from the calculated value at 0 m and the slope of the decrease in the measured  $\delta^{15}\text{N-NH}_4^+$  values at downstream stations (see text for explanation). All values are background-corrected but not corrected for regeneration. NA = data not available

Sampling Station (m)	Day 0		Day 20		Day 41		Day 1 post Measured
	Measured	Corrected	Measured	Corrected	Measured	Corrected	
0	227.3 <sup>a</sup>	319.4 <sup>b</sup>	289.6 <sup>a</sup>	370.9 <sup>b</sup>	306.1	661.9 <sup>b</sup>	—
116	236 <sup>c</sup>	—	321 <sup>c</sup>	—	263	568	3.2
176	198	278	236	302	240	520	NA
251	192	269	230	294	234	507	5.3
301	182	255	215	276	243	526	5.0
351	173	243	208	266	216	467	9.8
396	170	239	198	253	207	448	9.1
461	162	227	178	228	170	367	NA

<sup>a</sup>Estimated from linear regression of the remaining measurements on distance.

<sup>b</sup>Calculated from dripper rate.

<sup>c</sup>Tracer appears to be incompletely mixed at this station so this value is not used in calculations.

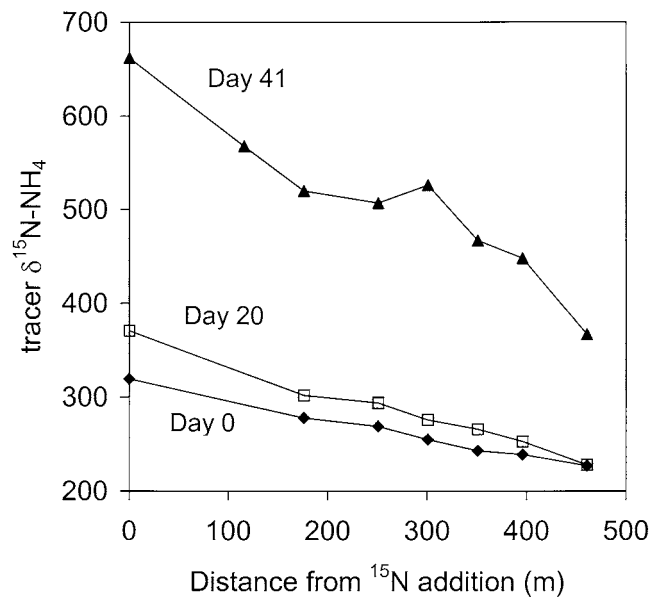


Figure 3. Longitudinal profiles of tracer  $\delta^{15}\text{N-NH}_4^+$  on days 0, 20, and 41 of the  $^{15}\text{N}$  addition. Values are corrected as shown in Table 3.

*Table 4.* Ammonium and nitrate uptake lengths and rates, estimated from the observed downstream change in  $\delta^{15}\text{N}$  during the  $^{15}\text{N}$  addition. Discharge and concentrations are means for the entire reach ( $N = 9$  measurements on each date). Residence times are calculated as uptake length divided by mean water velocity; the velocity was assumed to remain the same as that measured on Day 0 (0.24 m/s). Uptake of  $\text{NO}_3^-$  was too low to have a measurable impact on streamwater concentrations and  $\delta^{15}\text{N}\text{-NO}_3^-$ , and thus the  $\text{NO}_3^-$  uptake length must have been much longer than the study reach

	Day 0	Day 20	Day 41
<b>Discharge (L/s)</b>	208	201	191
<b><math>\text{NH}_4^+</math>:</b>			
Concentration ( $\mu\text{g N/L}$ )	23.4	21.3	12.4
Flux ( $\mu\text{g N/s}$ )	4867	4281	2368
Uptake length (m)	1349	932	766
(95% C.I.)	(1152–1629)	(719–1325)	(438–3040)
Residence time (min)	94	65	53
Total uptake rate ( $\mu\text{g N m}^{-2} \text{ min}^{-1}$ )	47.1	59.9	40.6
Nitrification ( $\mu\text{g N m}^{-2} \text{ min}^{-1}$ )	22.8	25.4	11.8
Assimilatory uptake ( $\mu\text{g N m}^{-2} \text{ min}^{-1}$ )	24.3	34.4	28.9
<b><math>\text{NO}_3^-</math>:</b>			
Concentration ( $\mu\text{g N/L}$ )	28.8	18.0	8.7
Flux ( $\mu\text{g N/s}$ )	5990	3618	1662
<b>DON:</b>			
Concentration ( $\mu\text{g N/L}$ )	150	193	287

tracer (Newbold et al. 1981). The apparent linear decrease probably reflects the short distance of the sampling transect relative to the  $\text{NH}_4^+$  uptake length in this stream; an exponential decline would likely have been observed if we could have sampled over a longer distance. The  $\text{NH}_4^+$  uptake lengths determined from longitudinal profiles of  $\delta^{15}\text{N}\text{-NH}_4^+$  changed from 1349 m on day 0 to 932 m on day 20 and 766 m on day 41, with more uncertainty in the estimates for the latter two dates (Table 4). In contrast, the whole-stream  $\text{NH}_4^+$  uptake rate, expressed on an areal basis, did not vary greatly across the three dates (Table 4). The shorter uptake lengths observed later in the experiment are probably explained by the decreasing discharge and  $\text{NH}_4^+$  concentration over this period, which reduced the  $\text{NH}_4^+$  flux and hence would have increased the relative impact of benthic uptake and transformation on the dissolved  $\text{NH}_4^+$ .

Nitrification accounted for a substantial fraction (29–48%) of the total  $\text{NH}_4^+$  uptake, with the lowest rate on day 41 coinciding with the lower  $\text{NH}_4^+$

Table 5. Longitudinal trends in  $\text{NO}_3^-$  concentration over the course of the  $^{15}\text{N}$  addition. N is the number of points sampled along the transects,  $\text{NO}_3^-$  concentrations are the means for all samples across the transects, and the regression slopes are given only when a significant downstream increase in concentration was observed (n.s. = not significant at  $P < 0.10$ )

Sampling Date	Day	N	$\text{NO}_3^-$ concentration ( $\mu\text{g N/L}$ )	Regression slope ( $\mu\text{g N L}^{-1} \text{m}^{-1}$ )
11-Jun-98	-5	10	28.8	0.0204
12-Jun-98 morning	-4	17	27.5	0.0104
12-Jun-98 afternoon	-4	9	29.1	n.s.
15-Jun-98	-1	5	29.7	n.s.
16-Jun-98	0	8	28.8	n.s.
23-Jun-98	7	7	19.7	0.0123
01-Jul-98	15	9	15.7	0.0079
06-Jul-98	20	5	18.1	0.0266
14-Jul-98	28	7	16.3	0.0199
27-Jul-98	41	4	8.7	n.s.
29-Jul-98	43	4	6.2	n.s.

N concentration in the stream. The nitrification rates expressed as a fraction of the available  $\text{NH}_4^+$  ( $k_N$ ), estimated from the increase in  $^{15}\text{NO}_3^-$  flux using the mass-balance model, were similar on the three measurement dates (mean,  $0.00040 \text{ m}^{-1}$ ). Indirect nitrification (i.e., the nitrification of  $^{15}\text{NH}_4^+$  that had been regenerated from biomass) was evidently not a substantial proportion of the total nitrification in Eagle Creek, as indicated by the relatively low  $\text{NH}_4^+$  regeneration rates estimated on day 1 post (see below). Assimilatory uptake of  $\text{NH}_4\text{-N}$ , as estimated from the difference between total uptake and nitrification, ranged between  $24\text{--}34 \mu\text{g m}^{-2} \text{min}^{-1}$  and did not decrease with the decrease in  $\text{NH}_4^+$  concentrations on day 41.

Longitudinal profiles of  $\text{NO}_3^-$  concentrations showed a detectable increase over the study reach on 6 of the 11 dates for which measurements are available (Table 5). This observation, together with the observed increase in the  $\delta^{15}\text{N}\text{-NO}_3^-$  over the study reach, suggest that uptake of  $\text{NO}_3^-$  from the stream water was too low to be detected (i.e.,  $k_2$  in Figure 1(a) and 1(b) was approximately zero). Nitrification of  $^{15}\text{NH}_4^+$  increased the flux of  $^{15}\text{NO}_3^-$  across the study reach, as shown by the longitudinal profiles and model fits in Figure 4. In the absence of uptake this nitrification should have increased the  $\text{NO}_3^-$  concentration, but evidently the increase was not large enough to be consistently detectable. The nitrification rates estimated from the  $^{15}\text{NO}_3^-$  profiles can

be compared to the rate of increase in  $\text{NO}_3^-$  concentration across the reach, for sampling dates when the  $\text{NO}_3^-$  increase was detectable. The mean of the six regression slopes in Table 5 is  $0.0163 \mu\text{g N L}^{-1} \text{m}^{-1}$ , which would yield a  $\text{NO}_3^-$  concentration increase of ca.  $7.5 \mu\text{g N/L}$  across the 460-m study reach. This apparent  $\text{NO}_3^-$  production rate is equivalent to  $39 \mu\text{g N m}^{-2} \text{min}^{-1}$ , which is almost twice the  $^{15}\text{N}$ -based nitrification estimate of ca.  $20 \mu\text{g N m}^{-2} \text{min}^{-1}$  (Table 4). The concentration increase could reflect groundwater inputs of  $\text{NO}_3^-$  as well as nitrification; although such inputs did not produce a measurable increase in discharge, even small quantities of groundwater could be significant sources of  $\text{NO}_3^-$  if groundwater concentrations are elevated relative to the stream. We sampled several shoreline seeps in the vicinity of the study reach and found  $\text{NO}_3^-$  concentrations to be highly variable, ranging from ca. 10 to 3,050  $\mu\text{g N/L}$ , with 6 of the 9 samples exceeding streamwater  $\text{NO}_3^-$  concentrations by at least 10-fold.

#### *Nitrogen regeneration rates*

Regeneration of  $^{15}\text{NH}_4^+$  from biomass compartments was detectable on the day after the addition ceased (day 1 post). The  $\delta^{15}\text{N-NH}_4^+$  ranged from 3–10‰ above background and increased in the downstream direction. In contrast, regeneration of  $\text{NO}_3^-$  was barely detectable; the  $\delta^{15}\text{N-NO}_3^-$  was variable along the reach and ranged from 0–5‰ above background. Application of the mass-balance model shown in Figure 1(c) yielded an estimate of  $k_r$ , the rate of  $^{15}\text{N}$  regeneration from biomass, of  $3.3 \times 10^{-7} \text{s}^{-1}$  for  $^{15}\text{NH}_4^+$  and  $< 3 \times 10^{-9} \text{s}^{-1}$  for  $^{15}\text{NO}_3^-$ . Re-uptake of the  $^{15}\text{NH}_4^+$  and  $^{15}\text{NO}_3^-$  (i.e.,  $k_2$  in Figure 1(c)) could not be detected across the study reach, and hence the  $k_r$  approximates the gross  $^{15}\text{N}$  regeneration rate in Eagle Creek.

#### *Nitrogen incorporation and turnover in organic matter*

The detrital and autotrophic organic matter compartments became measurably enriched in  $^{15}\text{N}$  during the 42-day addition, and subsequently decreased to near background levels during the 28 days after completion of the addition (Figure 5). Consistent downstream trends in  $\delta^{15}\text{N}$  were not detected in the organic matter compartments, so data have been averaged across the study reach in Figure 5. Epilithon became most enriched, reaching a mean  $\delta^{15}\text{N}$  of 155‰ above background by Day 42 (Figure 5), yet this was well below the  $\delta^{15}\text{N-NH}_4^+$  during the addition. Leaves and wood reached 20–30‰ with large spatial variability. Isotopic enrichment was smaller but measurable in the fine particulate organic matter in bottom deposits (FBOM) and in the water column (SPOM). The most  $^{15}\text{N}$ -enriched organic matter that we found in the stream included two samples of the filamentous alga *Cladophora glomerata*



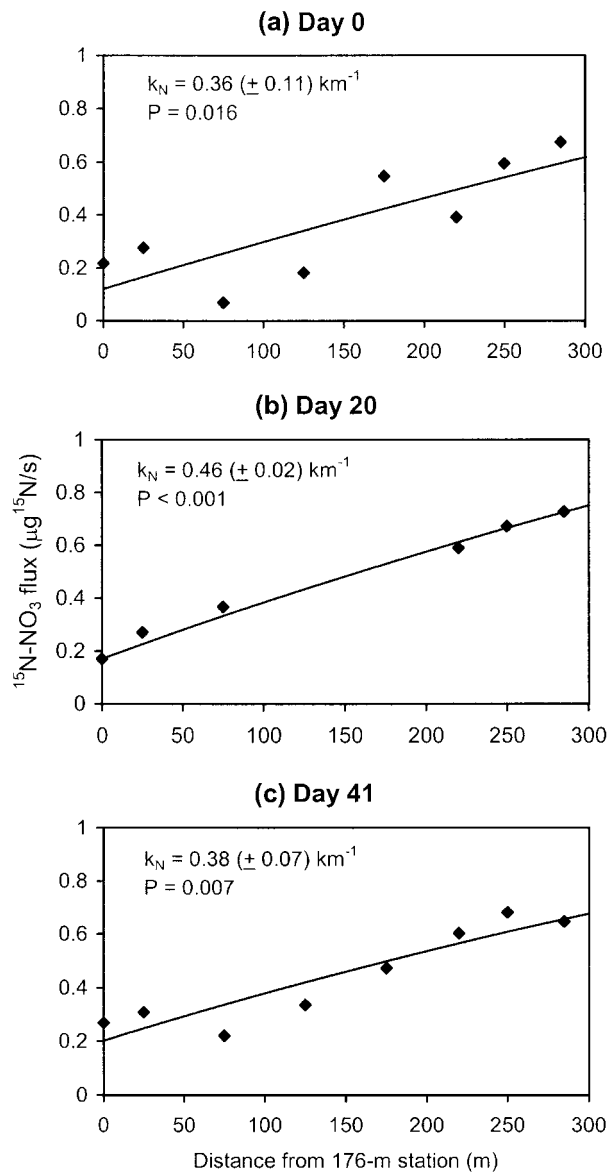


Figure 4. Measured flux rates of  $^{15}\text{NO}_3^-$  (symbols) and the nitrification rates ( $k_N$ ; S.E. in parentheses) estimated from the flux profiles using the models depicted in Figures 1(a) and 1(b). Lines depict cumulative nitrification.

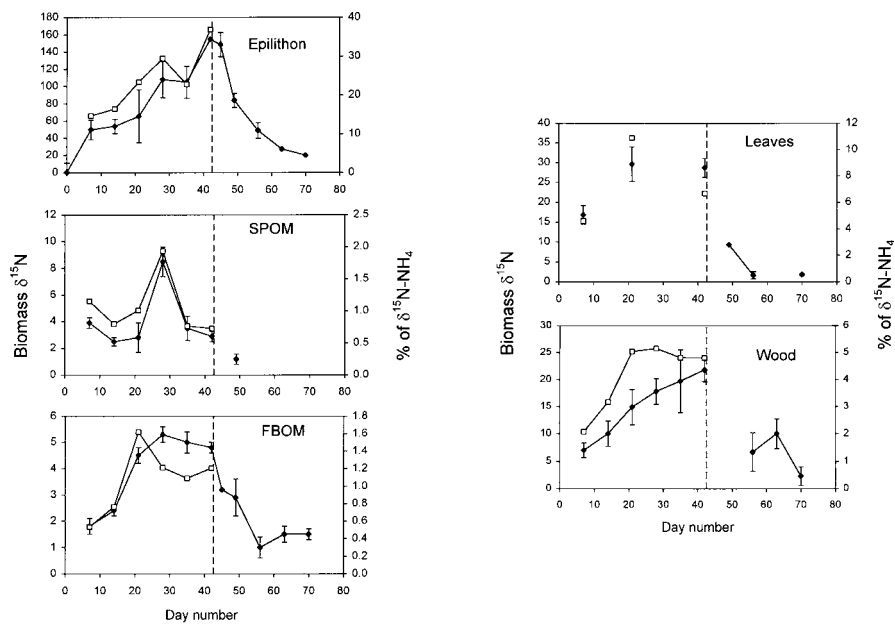


Figure 5. Temporal patterns of  $^{15}\text{N}$  enrichment in organic matter compartments during and after the addition of  $^{15}\text{NH}_4^+$  to the stream. The vertical dashed line marks day 42, when the  $^{15}\text{N}$  addition ceased. The solid circles show the mean tracer  $\delta^{15}\text{N}$  across the study reach, with bars showing standard errors of the means. The hollow squares show the percentage of biomass  $\delta^{15}\text{N}$  relative to the  $\delta^{15}\text{N-NH}_4^+$  averaged over the  $^{15}\text{N}$  turnover time of the biomass, which provides an indication of whether the biomass N reached isotopic steady state with streamwater  $\text{NH}_4^+$ . In most cases, there are  $\delta^{15}\text{N}$  measurements for all seven stations on days 7 and 42 and for three stations (usually 116, 301, and 461 m) on the other dates. Although spatial variability was observed along the study reach, the  $\delta^{15}\text{N}$  of samples from all sampling stations on days 7 and 42 showed no significant decrease in enrichment in the downstream direction, and therefore measurements from all stations have been pooled.

that appeared on rocks at 461 m during the latter part of the  $^{15}\text{N}$  addition period; they were collected on day 42 and measured 278 and 309‰ (not background-corrected). Among the invertebrates, larvae of the mayfly *Baetis* were most enriched, ranging between 160 and 340‰ on days 35 and 42 (background-corrected). These high  $^{15}\text{N}$  enrichments in biomass support the validity of our correction of the measured  $\delta^{15}\text{N-NH}_4^+$  values in Table 3.

Estimates of turnover rates of N in the primary uptake compartments are provided in Table 6. Turnover rates can be estimated in two ways, both of which assume that the organic matter is at steady state with regard to nitrogen uptake and loss. One way is to compare the  $^{15}\text{NH}_4^+$  uptake by a particular compartment during the first seven days of the  $^{15}\text{N}$  addition to the total nitrogen in that compartment, which yields an ‘apparent turnover rate’ for

N. The other way is to estimate the  $^{15}\text{N}$  turnover rate from the decline in  $\delta^{15}\text{N}$  in the compartment over the 28 days after the addition ceased (Figure 5). If all of the nitrogen in the compartment were actively cycling, these two estimates should agree. Table 6 shows that the turnover rates estimated from loss of tracer  $^{15}\text{N}$  were faster than the apparent N turnover rates based on uptake, which indicates that only a fraction of the total N in the compartment was actively cycling. Leaves had the fastest  $^{15}\text{N}$  turnover, followed by FBOM. Epilithon and wood showed somewhat longer  $^{15}\text{N}$  turnover times, although the estimate for wood is not statistically significant. The difference in turnover rate estimates by the two approaches provides an indication of the relative fraction of the total N that is actively turning over in each compartment (Tank et al. 2000).

The degree of enrichment in the  $\delta^{15}\text{N-NH}_4^+$  was variable throughout the  $^{15}\text{N}$  addition (Figure 2(d)), and the various organic matter compartments would have approached N isotopic steady-state at different rates because they differ in their N turnover times. The ratio of the  $\delta^{15}\text{N}$  in a primary uptake compartment to the mean  $\delta^{15}\text{N-NH}_4^+$  over a preceding interval equal to the  $^{15}\text{N}$  turnover time of that compartment provides an approximate indication of whether the organic matter compartment had reached isotopic steady-state. We accounted for the observed downstream decrease in  $\delta^{15}\text{N-NH}_4^+$  (Figure 3) in the calculation of these mean  $\delta^{15}\text{N-NH}_4^+$  values. These comparisons are expressed as percentages in Figure 5, and show that these compartments did appear to be approaching isotopic steady-state, as would be expected based on the estimated turnover times. However, none of the compartments approached the  $\delta^{15}\text{N-NH}_4^+$  during the experiment; epilithon came closest, reaching 37% by day 42.

Additional measurements of isotopic enrichment of leaves and wood are available from the incubation experiment (Figure 6). In contrast to the leaves and woody debris that we sampled from the stream bottom, these were samples of relatively fresh material of known origin that had been pre-conditioned in the stream and were maintained in one place throughout the experiment. The exclusion of sunlight had no consistent effect on the isotopic enrichment of these detrital samples, indicating that attached algal growth contributes little to the isotopic enrichment of detritus. The White Oak and Beech leaves became slightly more enriched than the leaves sampled from the stream bottom. Biofilm scrapings from the Oak dowel became considerably more enriched than the woody debris sampled from the stream bottom, perhaps because the debris samples included a higher proportion of the original wood than the scrapings.

The ratios of  $\delta^{15}\text{N}$  in the biomass to the mean  $\delta^{15}\text{N}$  for the turnover period, which are plotted in Figure 6 as percentages, suggest that the leaves

Table 6.  $\text{NH}_4^+$  uptake and N turnover rates. Uptake rates were determined for days 0–7 using equation 3, and are means for all stations with ranges in parentheses. Division of the  $\text{NH}_4^+$  uptake rate by the total N in the compartment yields the N-specific  $\text{NH}_4^+$  uptake, and its inverse is the apparent N turnover time (assuming all N in the compartment is actively cycling). Turnover rates of tracer  $^{15}\text{N}$  were estimated from the observed decline in  $\delta^{15}\text{N}$  after termination of the  $^{15}\text{N}$  addition (Figures 5 and 6). Estimates are significant at  $P = 0.05$  unless noted;  $^{15}\text{N}$  turnover for the incubated samples was estimated from only two sampling dates (day 41 and day 7 post)

Compartment	Day 0–7 $\text{NH}_4^+$ uptake rate ( $\text{mg N m}^{-2} \text{d}^{-1}$ )	Day 0–7 N-specific $\text{NH}_4^+$ uptake rate ( $\text{mg N mg N}^{-1} \text{d}^{-1}$ )	Day 0–7 Apparent N turnover time (d)	Post-addition $^{15}\text{N}$ turnover rate ( $\text{d}^{-1}$ )	Post-addition $^{15}\text{N}$ turnover time (d)
Epilithon	7.91 (2.55–12.95)	0.026	38	0.075	13.3
FBOM	7.10 (3.83–12.30)	0.0012	833	0.138	7.2
Small woody debris	9.41 (4.69–16.60)	0.0036	278	0.046 <sup>a</sup>	21.8 <sup>a</sup>
Leaves	0.41 (0.26–0.60)	0.014	71	0.222	4.5
Incubated Oak dowel	—	—	—	0.021	47.8
Incubated White Oak leaves	—	—	—	0.113	8.8
Incubated Black Oak leaves	—	—	—	0.132	7.6
Incubated Beech leaves	—	—	—	0.081	12.3

<sup>a</sup> $P = 0.18$ .

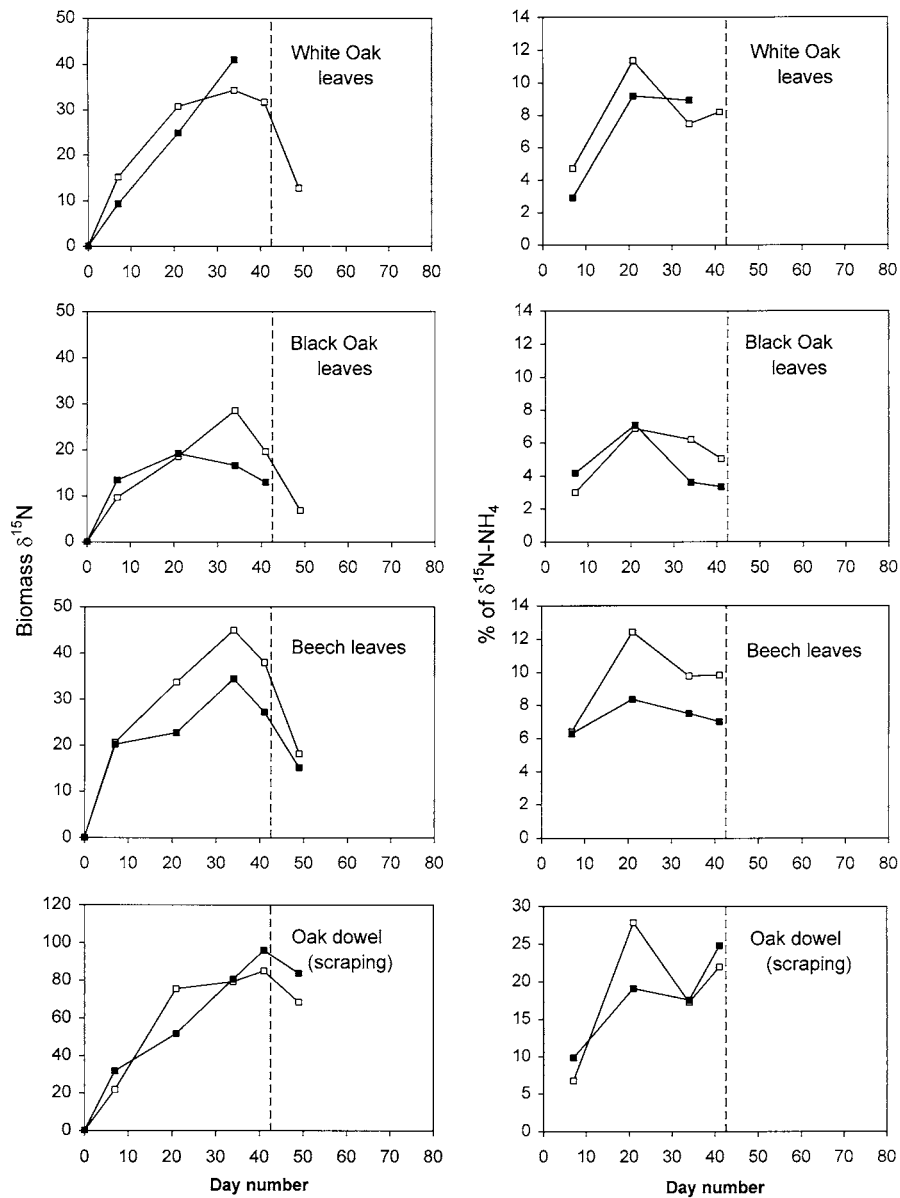


Figure 6. Temporal patterns of  $^{15}\text{N}$  enrichment in leaves and wooden dowels that were incubated in the stream during the experiment. The vertical dashed line marks day 42, when the  $^{15}\text{N}$  addition ceased. Solid and hollow symbols show data from incubations in the dark and light, respectively. Panels on the left show tracer  $\delta^{15}\text{N}$  and panels on the right show the ratio of biomass  $\delta^{15}\text{N}$  to the mean  $\delta^{15}\text{N-NH}_4^+$  over the  $^{15}\text{N}$  turnover time of the biomass, which provides an indication of whether the biomass N reached isotopic steady state with streamwater  $\text{NH}_4^+$ .

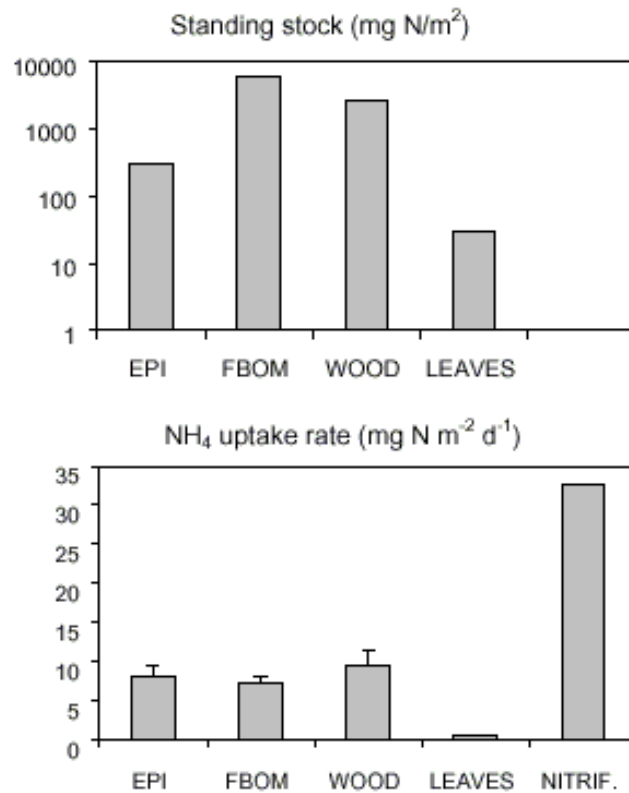


Figure 7. N standing stocks and NH<sub>4</sub><sup>+</sup> uptake rates in specific compartments (Days 0–7; means for all stations with standard errors). Compartment uptake rates are based on the observed enrichment in <sup>15</sup>N by Day 7 (see equation 3 and Table 6). The nitrification rate estimated for day 0 is included for comparison.

had reached isotopic steady-state, but the Oak dowel may not have. Table 6 shows that the turnover times for the material in the incubation experiment were longer than the estimates for leaves and wood on the stream bottom. However, turnover was estimated from composite samples collected on just two sampling dates (day 42 and day 8 post) because after day 8 post the samples began to break apart.

Ammonium uptake rates for each compartment were estimated for the initial 7 days of the <sup>15</sup>N addition using equation 3 (Figure 7 and Table 6). Epilithon, wood, and FBOM were each important to the total NH<sub>4</sub><sup>+</sup> uptake in the stream, despite their large differences in N standing stock. Leaves had a much lower standing stock and were less important in overall NH<sub>4</sub><sup>+</sup> uptake. The rate of transformation of NH<sub>4</sub><sup>+</sup> to NO<sub>3</sub><sup>-</sup> by nitrification was slightly greater than the total assimilation rate by the primary uptake compartments.

The sum of assimilative uptake and nitrification ( $57.7 \text{ mg N m}^{-2} \text{ d}^{-1}$ ) was 85% of the total  $\text{NH}_4^+$  uptake as estimated from the downstream decline in  $\delta^{15}\text{N-NH}_4^+$  on day 0 of the  $^{15}\text{N}$  addition ( $67.8 \text{ mg N m}^{-2} \text{ d}^{-1}$ ).

#### *Tracer $^{15}\text{N}$ in the algal fraction of epilithon*

The algal fraction of epilithon separated by density-gradient centrifugation on day 32 was biochemically and isotopically distinct from the bulk material scrubbed from rock surfaces (Figure 8). The mass ratio of carbon to chlorophyll-*a* (C:Chl) provides an indication of the amount of algal material in the samples relative to other organic matter. Studies of freshwater phytoplankton have shown that the C:Chl ratio of algal biomass is often around 50 or less (Reynolds 1984; Riemann et al. 1989). The C:Chl data in Figure 8 indicate that the algal fraction was composed primarily of live algae, whereas the bulk material contained variable amounts of additional organic matter that was either detritus derived from algae or some other organic matter. Five of the 6 samples of the algal fraction showed a narrow range of C:Chl ratios (37–45). Assuming that the C:Chl ratio in the algal fraction represents pure algae, algal biomass comprised about 48–84% of the total organic matter in the six bulk epilithon samples (mean, 70%). Algal cell counts in two samples showed that the algal fraction was dominated by cyanobacteria (91% of the total cells), with chlorophytes comprising most of the remainder. The  $\delta^{15}\text{N}$  of the algal fraction of epilithon was consistently higher than that of the bulk material (Figure 8), indicating that our bulk epilithon  $\delta^{15}\text{N}$  measurements underestimate the  $\delta^{15}\text{N}$  of epilithic algae, as expected if the bulk material contains some detrital organic matter.

The mean C:Chl ratio for bulk epilithon samples taken across the study reach just prior to the  $^{15}\text{N}$  addition was 165 (Table 1), which is higher than the ratios in Figure 8. Assuming a C:Chl ratio of 40 for the algal fraction, the mean fractional algal biomass in epilithon for the entire study reach would be estimated at ca. 24%. The two stations selected for collection of the algal fraction of epilithon were riffles, where less detrital organic matter may have accumulated on the rocks due to the faster current.

#### *Total retention of $^{15}\text{N}$ during the experiment*

The total mass of  $^{15}\text{N}$  retained within the 461-m study reach by the end of the addition period (day 42) was 1414 mg, or 6.7% of the total  $^{15}\text{N}$  added as  $\text{NH}_4^+$  over the course of the addition (Table 7). The remainder of the added  $^{15}\text{N}$  can be accounted for through export from the study reach, mainly in the form of  $\text{NH}_4^+$ , although the export of tracer  $^{15}\text{N}$  in  $\text{NO}_3^-$ , DON, and SPOM was also significant. The sum of estimated retention and export slightly exceeds the

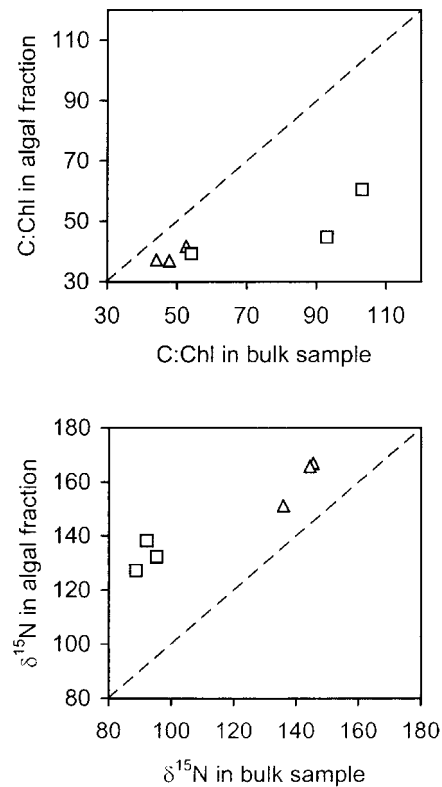


*Figure 8.* Comparison of C:Chl mass ratios and  $\delta^{15}\text{N}$  in bulk epilithon and the algal fraction of the epilithon that was separated from the bulk material by density-gradient centrifugation in colloidal silica. Samples were collected on day 32 of the  $^{15}\text{N}$  addition from two stations. The squares depict samples from 351 m and triangles depict samples from 461 m, and the dashed line shows the 1:1 relationship.

quantity of  $^{15}\text{N}$  added over the course of the addition, which likely reflects uncertainties in the estimates of flux due to temporal variability in discharge and  $\text{NH}_4^+$  concentrations.

The primary uptake compartments – epilithon, FBOM, wood, and leaves – accounted for 97% of the  $^{15}\text{N}$  retained in the study reach. Epilithon, FBOM, and wood contained approximately equal amounts of  $^{15}\text{N}$ , while leaves accounted for much less retention. Retention of  $^{15}\text{N}$  in the consumers was a small proportion of the total retention, as expected given their small relative biomass. Insect larvae, amphipods, and adult crayfish accounted for most of the retention by consumers. The unionid bivalves retained little  $^{15}\text{N}$  despite their large contribution to total consumer biomass (Table 1), reflecting their slow turnover rates (Raikow & Hamilton 2001).



Table 7. Mass balance of  $^{15}\text{N}$  at the end of the  $^{15}\text{N}$  addition (Day 42), for the 461-m study reach. The total mass of  $^{15}\text{N}$  added to the stream over the 42 days was 21,090 mg

Compartment	$^{15}\text{N}$ (mg)	% of added $^{15}\text{N}$
Epilithon	464	2.20
FBOM (upper cm)	437	2.10
Small woody debris	468	2.20
Leaves	8	0.04
Sum of primary uptake compartments	1377	6.50
Benthic insects, amphipods	16.6	0.080
Crayfish	14.9	0.070
Unionid bivalves	1.6	0.008
Fishes	4.3	0.020
Sum of consumers	37.4	0.180
$^{15}\text{NH}_4^+$ export	13,811	65.5
$^{15}\text{NO}_3^-$ export	2,788	13.0
$^{15}\text{N}$ -DON export	2,154	10.2
$^{15}\text{N}$ export as SPOM	1,799	8.5
Sum of $^{15}\text{N}$ export	20,552	97.5
Sum of retention and export	21,966	104

## Discussion

The results of this  $^{15}\text{N}$  tracer study in Eagle Creek are of particular interest for several reasons. As a woodland stream in a temperate humid climate, Eagle Creek represents the type of stream that has been most frequently studied and hence has shaped our conceptual views of lotic ecology (Cummins et al. 1981; Minshall et al. 1983; Allan 1995). The present experiment provides an opportunity to validate concepts of stream nutrient cycling that were originally developed from other lines of evidence, such as the predominance of heterotrophic microbial activity in shaded stream channels (Minshall et al. 1983), as well as the importance of food webs sustained by vascular-plant detritus (Cummins & Klug 1979). Eagle Creek is also typical of watersheds in the eastern U.S. that are experiencing elevated N loading, and the present study provides insights into how stream ecosystems respond to N inputs. Comparable  $^{15}\text{N}$  enrichment studies that have been reported in the literature

so far include experiments in the Kuparuk River system of the Alaskan tundra (Peterson et al. 1997) and in much smaller, montane forest streams in North Carolina (Hall et al. 1998; Tank et al. 2000) and Tennessee (Mulholland et al. 2000). Eagle Creek is interesting to compare with those studies because it carries higher concentrations of nutrients, and unlike the montane streams, it is a relatively low-gradient stream that is influenced by wetlands along its course.

#### *N uptake rates and lengths*

The relatively long uptake lengths of  $\text{NH}_4^+$  in Eagle Creek (Table 4) compared to most streams for which estimates are available is explained by the combination of higher discharge and higher  $\text{NH}_4^+$  concentrations in Eagle Creek. When expressed on an areal basis, uptake rates of  $\text{NH}_4^+$  are of the same order as rates measured in much smaller streams covered by forest canopy, where uptake lengths are  $< 100$  m (Mulholland et al. 2000; Tank et al. 2000). Thus the rate of N uptake and transformation by benthic metabolism in Eagle Creek resembles rates measured in the smaller streams, and is evidently controlled by factors other than water depth and discharge. Smaller streams are likely to have greater effects on streamwater nitrogen concentrations due to greater contact of water with benthic detritus, biofilms, and sediments. Greater depth and velocity in the water column overlying the stream bottom will result in less impact of the benthic biota on advective nutrient fluxes. Nutrient assimilation may be lowest in shaded streams like Eagle Creek during the summer despite the higher water temperatures because leaf litter inputs from the previous autumn are largely decomposed by June (Suberkropp & Klug 1976), and shading by the deciduous forest canopy over the stream limits aquatic primary production (Cummins et al. 1981; King 1982).

Despite the long  $\text{NH}_4^+$  uptake length, N uptake and transformation within the stream channel significantly alter the form of N transported by the stream over distances of several kilometers. This level of biological influence on N transport probably represents the lower end of the range for streams of this size, considering that this stream (1) was formerly straightened by channelization and has little connectivity with its floodplain in the study reach, (2) has a largely sandy bottom that is an unstable substratum for algal colonization, and (3) has low aquatic primary production because the stream channel is mostly shaded by surrounding forest. However, this kind of stream is common throughout eastern North America, and such streams frequently pass through wetlands that could be sources of  $\text{NH}_4^+$  to downstream waters, as in the case of Eagle Creek, or they may receive  $\text{NH}_4^+$  from pollution inputs.

The study reach for this experiment would ideally have been much longer so it would encompass several  $\text{NH}_4^+$  uptake lengths, as has been the case in

the experiments performed in small streams (e.g., Mulholland et al. 2000). Unfortunately, the length of our study reach was constrained by beaver ponds upstream and the confluence of the creek with the Kalamazoo River downstream. In this region, it would be difficult to find such a long reach that did not include substantial hydrologic inputs and geomorphological variability, which would complicate the interpretation of  $^{15}\text{N}$  addition experiments. The stable isotope tracer approach allowed us to estimate  $\text{NH}_4^+$  uptake in the reach, whereas uptake could not be quantified over such a short distance using short-term  $\text{NH}_4^+$  additions.

#### *Relative importance of $\text{NH}_4^+$ and $\text{NO}_3^-$ assimilation*

On the basis of empirical evidence as well as thermodynamic considerations, algae and heterotrophic bacteria and fungi are expected to exhibit a preference for assimilation of  $\text{NH}_4^+$  when both  $\text{NH}_4^+$  and  $\text{NO}_3^-$  are available (Reynolds 1984; Fenchel et al. 1998). In Eagle Creek both of these nitrogen forms were present at relatively high concentrations during the addition (Figure 2) and in the preceding months, and thus  $\text{NH}_4^+$  should be the primary form of N that is assimilated from the stream water.  $\text{NH}_4^+$  uptake was measurable but uptake of  $\text{NO}_3^-$  could not be detected in the study reach, which is consistent with a preference for  $\text{NH}_4^+$  assimilation by the stream biota.

Heterotrophic bacteria and fungi that decompose particulate organic matter in Eagle Creek would be expected to assimilate nitrogen from the water because the detrital material on which they subsist has high C:N ratios (Suberkropp & Klug 1976; Suberkropp & Chauvet 1995; Caraco et al. 1998). Dissolved organic matter in the stream was also relatively low in N, with a DOC:DON mass ratio of approximately 20 at the start of the experiment. Neither heterotrophic fungi nor algae responded to N in the nutrient-diffusing substrata experiments, indicating that microbes in biofilms were likely not N-limited. Therefore heterotrophic microbes could become as labeled with  $^{15}\text{N}$  as algae if both relied primarily upon streamwater  $\text{NH}_4^+$  to support growth. Results from the dark incubations of detrital organic matter showed that heterotrophic uptake of  $\text{NH}_4^+$  was significant, and this uptake was evidently due to microorganisms in the detritus rather than algae.

If  $\text{NH}_4^+$  is the preferred N source, algae and heterotrophic microbes with rapid turnover rates should have approached the  $\delta^{15}\text{N}$  of the  $\text{NH}_4^+$  over the course of the 42-day  $^{15}\text{N}$  addition, yet we did not find any organic compartments that approached the mean  $\delta^{15}\text{N}$ - $\text{NH}_4^+$  over periods corresponding to their  $^{15}\text{N}$  turnover times (Figures 5, 6). The bulk detrital samples collected in this study represent mixtures of living organisms (especially bacteria and fungi) and nonliving detrital organic matter (Cummins & Klug 1979), and N in the detrital organic matter likely obscured the accumulation of  $^{15}\text{N}$  in algal

and microbial biomass. Our measurements of  $\delta^{15}\text{N}$  in algae collected from bulk epilithon show how the living biomass can be much more enriched in  $^{15}\text{N}$  than the detrital organic matter in which these organisms dwell. Likewise, in other  $^{15}\text{N}$  enrichment studies of streams, autotrophs and detrital compartments generally did not approach the enrichment of the  $\text{NH}_4^+$  pool. This low degree of enrichment has been attributed to the assimilation of less-enriched  $\text{NO}_3^-$ , which was considerably more abundant than  $\text{NH}_4^+$  in those streams (Peterson et al. 1997; Mulholland et al. 2000), or to the presence of substantial N in the bulk material that was not actively cycling (Tank et al. 2000). In their  $^{15}\text{N}$  addition experiment in the Kugaruk River, however, Peterson et al. (1997) found that the  $\delta^{15}\text{N}$  of nearly pure samples of filamentous algae did approach the  $\delta^{15}\text{N}$ - $\text{NH}_4$ .

The  $\delta^{15}\text{N}$  of the algal material that was separated from the bulk epilithon can be compared to the  $\delta^{15}\text{N}$  of  $\text{NH}_4^+$  and  $\text{NO}_3^-$  to ascertain the relative contributions of these two N sources (Mulholland et al. 2000), but this comparison assumes that the entire N content of the algae was actively turning over during the  $^{15}\text{N}$  addition. The mean calculated  $\delta^{15}\text{N}$ - $\text{NH}_4^+$  for the 13 d prior to the sampling on day 32 (equivalent to the turnover rate for epilithon  $^{15}\text{N}$ ) was 625‰ at 0 m, which would correspond to approximately 455‰ at 351 m and 389‰ at 461 m, the two sites from which epilithic algae were collected. The C:Chl ratios indicated that the algal fractions contained nearly pure algae (Figure 8). The algal  $\delta^{15}\text{N}$  did not approach that of the streamwater  $\text{NH}_4^+$ , even though the turnover rate indicates that the algae should have reached isotopic equilibrium with N sources. An isotopic mixing model can be applied to estimate the relative importance of  $\text{NH}_4^+$  and  $\text{NO}_3^-$ , solving the following two equations simultaneously:

$$\delta^{15}\text{N}_{\text{biomass}} = (f_{\text{NH}_4})(\text{mean } \delta^{15}\text{N} - \text{NH}_4^+) + (f_{\text{NO}_3})(\text{mean } \delta^{15}\text{N} - \text{NO}_3^-) \quad (9)$$

$$f_{\text{NH}_4} + f_{\text{NO}_3} = 1 \quad (10)$$

where  $f_{\text{NH}_4}$  and  $f_{\text{NO}_3}$  refer to the relative fractions of N assimilated as  $\text{NH}_4^+$  and  $\text{NO}_3^-$ , respectively. Using the mean  $\delta^{15}\text{N}$ - $\text{NH}_4^+$  values given above and the mean  $\delta^{15}\text{N}$ - $\text{NO}_3^-$  for days 20 and 41 (27‰), this model estimates that the fractional  $\text{NH}_4^+$  assimilation averaged 32% for the 6 epilithic algal samples (range, 25–40%), suggesting that the majority of the assimilated N was  $\text{NO}_3^-$  rather than  $\text{NH}_4^+$ . This conclusion is unexpected for Eagle Creek, where N availability was apparently not limiting to algae and heterotrophs, and  $\text{NO}_3^-$  was not significantly more abundant than  $\text{NH}_4^+$ .

An alternative explanation for these results, which could also apply to the other  $^{15}\text{N}$  tracer studies in streams, is that a large fraction of the algal biomass was not actively cycling during the experiment. In this case the  $\delta^{15}\text{N}$  could

Table 8. Estimation of the fraction of actively cycling N ( $f_{\text{ACTIVE}}$ ) in organic matter compartments on day 35 of the  $^{15}\text{N}$  addition, and comparison with independent measurements of the N in algal or microbial biomass within the compartments. The active fraction was calculated with equation 11, assuming that all N is assimilated as  $\text{NH}_4^+$  from stream water. The measured microbial fraction ( $f_{\text{MICROBIAL}}$ ) represents either the algal C fraction in epilithon, as estimated from C:Chl ratios of bulk epilithon and its separated algal fraction (see Results), or the microbial N fraction in detritus, as extracted by chloroform fumigation (see Table 2). All data are means for multiple sites across the study reach

Biomass Compartment	$\delta^{15}\text{N}_{\text{BIOMASS}}$ on day 35	Mean $\delta^{15}\text{N-NH}_4$	Calculated $f_{\text{ACTIVE}}$	Measured $f_{\text{MICROBIAL}}$
Epilithon	104.9	462	0.230	0.240
FBOM	5.0	459	0.011	0.012
Wood	19.7	410	0.048	0.046
Leaves	28.7 <sup>a</sup>	432 <sup>a</sup>	0.066	0.080

<sup>a</sup>Means for Day 42 since leaves were not sampled on day 35.

still approach isotopic steady-state over the course of the  $^{15}\text{N}$  addition, but it would plateau at a much lower level due to the presence of relatively inactive algal nitrogen. For bulk epilithon samples, this inactive biomass N would augment the relatively inactive N contained in detrital organic matter. If the relatively low degree of  $^{15}\text{N}$  enrichment of bulk epilithon can be explained by a small fraction of algal biomass that assimilates  $\text{NH}_4^+$  within a large fraction of inactive N, then the fraction of actively cycling N ( $f_{\text{ACTIVE}}$ ) can be estimated by the following mixing model:

$$\delta^{15}\text{N}_{\text{biomass}} = (f_{\text{ACTIVE}})(\text{mean } \delta^{15}\text{N} - \text{NH}_4) \quad (11)$$

Table 8 shows these calculations for day 35, the sampling date that best coincides with our measurements of algal N in epilithon (day 32). The fraction of actively cycling algal N (23%) agrees closely with the fraction of algal N in epilithon (24%) estimated from C:Chl ratios, and therefore assimilation of  $\text{NH}_4^+$  by the algal fraction can account for the observed  $^{15}\text{N}$  enrichment of the bulk epilithon compartment. The presence of substantial quantities of relatively inactive algal biomass in Eagle Creek during the summer is conceivable because conditions for algal growth would have been better during the preceding spring (King 1982; Minshall et al. 1983).

Similar calculations for microbial N in FBOM, wood, and leaves on day 36 also reveal good agreement between the calculated active fraction, assuming uptake of  $\text{NH}_4^+$ , and the microbial fraction as estimated from the N released in chloroform fumigations (Table 8). We conclude from this analysis that there is no evidence for significant  $\text{NO}_3^-$  assimilation by the biota in Eagle Creek,

which agrees with our interpretation of the longitudinal profiles of  $\text{NO}_3^-$  concentrations and  $\delta^{15}\text{N}-\text{NO}_3^-$ . The patterns of  $^{15}\text{N}$  enrichment that we have observed can be explained by assimilation of  $\text{NH}_4^+$  by epilithic algae or by bacteria and fungi associated with particulate organic detritus, together with the fact that these living organisms comprise a minority of the total organic matter (and N) in our bulk samples of epilithon, FBOM, woody debris, and leaves.

These conclusions showing a relatively small actively cycling fraction of N in epilithon and organic detritus have important implications for studies of stream food webs. For example, standing stocks of epilithon are often evaluated on the basis of bulk C or chlorophyll contents, and these stocks are assumed to be available to consumers and to turn over rapidly, when in fact only a minority of that material may be growing rapidly and supporting much of the food web. Another implication of a protracted turnover rate is that standing stocks could represent antecedent conditions rather than those at the time of sampling, confounding attempts to correlate algal biomass with environmental factors. The interpretation of natural-abundance isotopic measurements made on bulk detrital and epilithon samples is often difficult because the samples are composed of unknown and variable mixtures of active and inactive organic components. Additional information on biochemical composition and microbial biomass can help explain observed patterns (Hamilton & Lewis 1992; Peterson et al. 1997; Tank et al. 2000).

#### *Assimilative $\text{NH}_4^+$ uptake compared with nitrification*

Whole-stream rates of nitrification and assimilative uptake of  $\text{NH}_4^+$  have infrequently been determined simultaneously, but results from Eagle Creek and the other LINX experiments show that nitrification can rival assimilative uptake as a sink for streamwater  $\text{NH}_4^+$ , and can significantly alter the form of N transported by streams (Peterson et al. 2001). Bacterial nitrification in streams occurs primarily in biofilms and the sediments (Stream Solute Workshop 1990), and requires oxygen as well as  $\text{NH}_4^+$ . Although the relative transient storage area of Eagle Creek is not particularly large ( $A_s:A = 0.25$ ), exchange between the transient storage zones and the stream water is rapid ( $\alpha = 0.002 \text{ s}^{-1}$ ). The coarse sand covering much of the bottom could maintain an oxic upper layer that provides optimal conditions for nitrification of  $\text{NH}_4^+$  that is continually resupplied by through-flowing stream water (Fenchel et al. 1998). The moderately high concentrations of  $\text{NH}_4^+$  in the stream water from upstream wetlands would allow nitrification to occur, while the limited light availability precludes much N uptake by autotrophs and the low inputs of allochthonous organic matter during the summer would limit demand for  $\text{NH}_4^+$  assimilation by heterotrophic microbes. Comparable areal rates of

nitrification have been measured in laboratory incubation studies of stream sediments (Kaushik et al. 1981). The conditions favoring nitrification in Eagle Creek could conceivably change at other times of the year, particularly when the stream receives high leaf litter inputs in the fall, increasing assimilative uptake by heterotrophic microbes (Mulholland et al. 1985; Tank et al. 2000).

The observation that a substantial fraction of the  $\text{NH}_4^+$  transported by the stream can be nitrified is particularly important because the resultant  $\text{NO}_3^-$  is then subject to denitrification during transport through the hydrologic system, which is the most important permanent sink for combined N en route to downstream ecosystems (Howarth et al. 1996). If the conditions in our reach were typical for the stream system, much of the  $\text{NH}_4^+$  from the upstream wetlands would be converted to  $\text{NO}_3^-$  within a few km, substantially increasing the  $\text{NO}_3^-$  concentration. It is possible that denitrification in the deeper sediments consumed  $\text{NO}_3^-$  from the overlying water column (Kaushik et al. 1981; Hedin et al. 1998), but the balance of evidence suggests that most of the nitrate that was produced accumulated in the stream water. Downstream in the river system the water passes through environments that are probably more conducive to denitrification and assimilative uptake, such as natural wetlands and floodplains as well as artificial impoundments, where nitrate could be removed at higher rates.

#### *Roles of heterotrophic and autotrophic organisms in N cycling*

The aquatic metabolism in Eagle Creek is predominantly heterotrophic during the summer, as shown by the diel metabolism study, and probably during the rest of the year as well since daytime dissolved  $\text{O}_2$  concentrations remain at or below atmospheric equilibrium. Ammonium oxidation by bacterial nitrification, a form of chemoautotrophic metabolism, can only account for ca. 1–3% of the  $\text{O}_2$  consumption rate in the creek, based on our estimates of nitrification rates and ecosystem respiration, and the  $\text{O}_2$  demand for complete nitrification to  $\text{NO}_3^-$  (Bansal 1977). The net heterotrophic metabolism of the creek is therefore explained by the high inputs of allochthonous organic matter originating from terrestrial vascular plants, which occur mainly during the autumn, combined with low light availability for aquatic primary production and the low stream gradient that permits considerable storage of organic matter on the stream bottom. As a consequence, heterotrophic microorganisms play an important role in N cycling in the creek, even during the summer when new organic matter inputs are relatively low. The relative abundance of bacteria and fungi in detrital organic matter in Eagle Creek (Table 2) is typical of forest streams during the summer, with bacteria dominating in FBOM and fungi dominating in wood and leaves (Allan 1995; Hall & Meyer 1998).

The in-situ incubations of detrital organic matter in the dark and the light showed that uptake of  $^{15}\text{N}$  by detrital compartments was due largely to heterotrophic microbes rather than attached algae (Figure 6). The high C:Chl ratios in detrital organic matter also support this conclusion (Table 1). Algae were not abundant enough in the sand or FBOM to be collected by the density-gradient centrifugation procedure, and hence significant growth of algae must be restricted to the hard surfaces of rocks and coarse woody debris.

Epilithon collected from cobble was the most  $^{15}\text{N}$ -enriched compartment that was sampled throughout the experiment (Figure 5), as has been observed in previous experiments (Peterson et al. 1997; Hall et al. 1998; Mulholland et al. 2000). The high enrichment of epilithon probably reflects the relatively high fraction of actively growing algal biomass in this material compared to the fraction of microbial N in the detrital organic matter. The nutrient-diffusing substrata experiments showed significant algal accumulation on the surfaces but no stimulatory effect of added N or P, suggesting that low light availability controlled algal growth. Greater algal growth could conceivably occur during the spring and fall, as was documented in forested reaches of nearby Augusta Creek by King (1982). The other organic matter compartments besides epilithon are primarily heterotrophic (Table 1), and together these heterotrophic compartments assimilate twice as much  $\text{NH}_4^+$  as the algae in epilithon (Figure 7).

## Conclusions

This study has produced a detailed understanding of N cycling in a forested stream, showing how inorganic N inputs are altered by assimilative uptake processes and dissimilative transformations mediated by algae and heterotrophic microbes. Allochthonous inputs of organic matter are processed by the stream biota, resulting in immobilization of streamwater  $\text{NH}_4^+$ , but a substantial fraction of the  $\text{NH}_4^+$  is also transformed to  $\text{NO}_3^-$  by nitrification. Algal production plays a smaller but not insignificant role in N uptake. Nitrate produced by nitrification is a less available form of N and accumulated in the stream water, but it is subject to permanent loss by eventual denitrification in downstream ecosystems. This whole-stream  $^{15}\text{N}$  enrichment study has provided an independent validation of many previously established concepts regarding N cycling in streams, and is unique in its comprehensive coverage and quantitative estimates of flux rates. The results for Eagle Creek offer an interesting addition to similar  $^{15}\text{N}$  tracer studies at other LINX sites because Eagle Creek is one of the largest streams studied and has greater nutrient availability, higher ratios of  $\text{NH}_4^+$  to  $\text{NO}_3^-$ , a lower gradient, and greater wetland influence.



## Acknowledgements

This experiment was accomplished with significant assistance from numerous people. Most of the methods and many of the ideas in this paper originated from stimulating meetings with the entire LINX project group. Field and laboratory work was carried out with assistance from M. Machavaram, E. Siler, J. Ervin, J. Halliday (under sponsorship by the government of New Zealand), N. Leonard (with NSF REU funds), J. Schaefer (REU), J. McCutchan, N. Dorn, J. Webster, E. Thobaben, A. Conklin, R. Sinsabaugh, and M. Osgood. S. Findlay analyzed the microbial samples, P. Mulholland assisted with calculations, K. Tholke and D. Birdsell assisted with isotopic analyses, S. Kohler and E. Siler identified invertebrates, D. Uzarski and C. Stricker electrofished, and R. Dufford enumerated algae. C. Kulpa of the Center for Environmental Science and Technology at the University of Notre Dame kindly allowed us to use their mass spectrometer facility. Financial support was provided by grants from the Ecosystems Program, National Science Foundation, to Virginia Polytechnic University (DEB-9628860) and to Michigan State University (DEB-9810220 and DEB-9701714). This is contribution 946 of the W.K. Kellogg Biological Station.

## References

- Alexander RB, Smith RA & Schwarz GE (2000) Effect of stream channel size on the delivery of nitrogen to the Gulf of Mexico. *Nature* 403: 758–761
- Allan JD (1995) *Stream ecology: Structure and Function of Running Waters*. Chapman and Hall, London
- Aminot A, Kirkwood DS & K  rouel R (1997) Determination of ammonia in seawater by the indophenol-blue method: Evaluation of the ICES NUTS I/C 5 questionnaire. *Mar. Chem.* 56: 59–75
- Bansal MK (1977) Nitrification in natural streams. *J. Wat. Pollut. Control Fed.* 48: 2380–2393
- Battaglin WA & Goolsby DA (1997) Statistical modeling of agricultural chemical occurrence in midwestern rivers. *J. Hydrol.* 196: 1–25
- Bencala KE & Walters RA (1983) Simulation of solute transport in a mountain pool-and-riffle stream: A transient storage model. *Water Resources Research* 19: 718–724
- Brookes PC, Kragt JF, Powlson DS & Jenkinson DS (1985a) Chloroform fumigation and the release of soil N: The effects of fumigation time and temperature. *Soil Biol. Biochem.* 17: 831–835
- Brookes PC, Landman A, Pruden G & Jenkinson DS (1985b) Chloroform fumigation and the release of soil N: A rapid direct extraction method to measure microbial biomass N in soil. *Soil Biol. Biochem.* 17: 837–842
- Cabrera ML & Beare MH (1993) Alkaline persulfate oxidation for determining total nitrogen in microbial biomass extracts. *Soil Sci. Soc. Am. J.* 57: 1007–1012

- Caraco NF, Lampman G, Cole JJ, Limburg KE, Pace ML & Fischer D (1998) Microbial assimilation of DIN in a nitrogen rich estuary: Implications for food quality and isotope studies. *Mar. Ecol. Prog. Ser.* 167: 59–71
- Caraco N & Cole JJ (1999) Human impact on nitrate export: An analysis using major world rivers. *Ambio* 28: 167–170
- Cummins KW & Klug MJ (1979) Feeding ecology of stream invertebrates. *Ann. Rev. Ecol. Syst.* 10: 147–172
- Cummins KW, Klug MJ, Ward GM, Spengler GL, Speaker RW, Ovink DC, Mahan DC & Petersen RC (1981) Trends in particulate organic matter fluxes, community processes and macroinvertebrate functional groups along a Great Lakes Drainage Basin river continuum. *Verh. Internat. Verein. Limnol.* 21: 841–849
- Fenchel T, King GM & Blackburn TH (1998) *Bacterial Biogeochemistry: The Ecophysiology of Mineral Cycling*. Academic Press, San Diego
- Fenn ME, Poth MA, Aber JD, Baron JS, Bormann BT, Johnson DW, Lemly AD, McNulty SG, Ryan DF & Stottleyer R (1998) Nitrogen excess in North American ecosystems: Predisposing factors, ecosystem responses, and management strategies. *Ecol. Applic.* 8: 706–733
- Galloway JN, Schlesinger WH, Levy H. II, Michaels A & Schnoor J (1995) Nitrogen fixation: Anthropogenic enhancement – environmental response. *Global Biogeochem. Cycles* 9: 235–252
- Goolsby DA (2000) Mississippi basin nitrogen flux believed to cause Gulf hypoxia. *Eos, Transactions, American Geophysical Union* 81: 321–327
- Grasshoff K, Ehrhardt M & Kremling K (Eds) (1983) *Methods of Seawater Analysis*. Verlag Chemie, Weinheim
- Hall RO Jr, Peterson BJ & Meyer JL (1998) Testing a nitrogen-cycling model of a forest stream by using a nitrogen-15 tracer addition. *Ecosystems* 1: 283–298
- Hall RO Jr & Meyer JL (1998) The trophic significance of bacteria in a detritus-based stream food web. *Ecology* 79: 1995–2012
- Hamilton SK & Lewis WM Jr (1992) Stable carbon and nitrogen isotopes in algae and detritus from the Orinoco River floodplain, Venezuela. *Geochim. Cosmochim. Acta* 56: 4237–4246
- Hart DR (1995) Parameter estimation and stochastic interpretation of the transient storage model for solute transport in streams. *Water Resources Res.* 31: 323–328
- Hedges JJ & Stern JH (1984) Carbon and nitrogen determination of carbonate-containing solids. *Limnol. Oceanogr.* 29: 657–663
- Hedin LO, Von Fisher JC, Ostrom NE, Kennedy BP, Brown MG & Robertson GP (1998) Thermodynamic constraints on nitrogen transformations and other biogeochemical processes at soil-stream interfaces. *Ecology* 79: 684–703
- Holmes R, McClelland W, Sigman DM, Fry B & Peterson BJ (1998) Measuring  $^{15}\text{N-NH}_4^+$  in marine, estuarine, and fresh waters: an adaptation of the ammonium diffusion method for samples with low ammonium concentrations. *Mar. Chem.* 60: 235–243
- Howarth RW, Billen G, Swaney D, Townsend A, Jaworski N, Lajtha K, Downing J, Elmgren R, Caraco N, Jordan T, Berendse F, Freney J, Kudeyarov V, Murdoch P & Zhao-Liang Z (1996) Regional nitrogen budgets and riverine N & P fluxes for the drainages to the North Atlantic Ocean: natural and human influences. *Biogeochemistry* 35: 75–139
- Kaushik NK, Robinson JB, Stammers WN & Whitely HR (1981) Aspects of nitrogen transport and transformation in headwater streams. In: Lock MA & Williams DD (Eds) *Perspectives in Running Water Ecology* (pp 113–139). Plenum Press, New York

- King DK (1982) Community metabolism and autotrophic-heterotrophic relationships of woodland stream riffle sections. Doctoral dissertation, Michigan State University (Kellogg Biological Station and Dept. of Fisheries and Wildlife), 356 pp
- Marzolf ER, Mulholland PJ & Steinman AD (1994) Improvements to the diurnal upstream-downstream dissolved oxygen change technique for determining whole-stream metabolism in small streams. *Can. J. Fish. Aquat. Sci.* 51: 1591–1599
- Minshall GW, Petersen RC, Cummins KW, Bott TL, Sedell JR, Cushing CE & Vannote RL (1983) Interbiome comparison of stream ecosystem dynamics. *Ecol. Monogr.* 53: 1–25
- Mueller DK & Helsel DR (1996) Nutrients in the Nation's Waters – Too Much of a Good Thing? USGS National Water-Quality Assessment Program Circular 1136
- Mulholland PJ, Newbold JD, Elwood JW, Ferren LA & Webster JR (1985) Phosphorus spiraling in a woodland stream: Seasonal variations. *Ecology* 66: 1012–1023
- Mulholland PJ, Steinman AD & Elwood JW (1990) Measurement of phosphorus uptake length in streams: comparison of radiotracer and stable PO<sub>4</sub> releases. *Can. J. Fish. Aquat. Sci.* 47: 2351–2357
- Mulholland PJ, Tank JL, Sanzone DM, Wollheim WM, Peterson BJ, Webster JR & Meyer JL (2000) Nitrogen cycling in a forest stream determined by a <sup>15</sup>N tracer addition. *Ecol. Monogr.* 70: 471–493
- Newbold JD, Elwood JW, O'Neill RV & Van Winkle W (1981) Measuring nutrient spiraling in streams. *Can. J. Fish. Aquat. Sci.* 38: 860–863
- Newell SY, Arsuffi TL & Fallon RD (1988) Fundamental procedures for determining ergosterol content of decaying plant material by liquid chromatography. *Appl. Environ. Microbiol.* 54: 1876–1869
- Peterson BJ, Wollheim WM, Mulholland PJ, Webster JR, Meyer JL, Tank JL, Martí E, Bowden WB, Valett HM, Hershey AE, McDowell WB, Dodds WK, Hamilton SK, Gregory S & Morrall DD (2001) Control of nitrogen export from watersheds by headwater streams. *Science* 292: 86–90
- Peterson BJ, Bahr M & Kling GW (1997) A tracer investigation of nitrogen cycling in a pristine tundra river. *Can. J. Fish. Aquat. Sci.* 54: 2361–2367
- Raikow DF & Hamilton SK (2001) Bivalve diets in a midwestern US stream: A stable isotope enrichment study. *Limnol. Oceanogr.* 46: 514–522
- Reynolds CS (1984) *The Ecology of Freshwater Phytoplankton*. Cambridge Univ. Press, Cambridge
- Riemann B, Simonsen P & Stensgaard L (1989) The carbon and chlorophyll content of phytoplankton from various nutrient regimes. *J. Plankton Res.* 11: 1037–1045
- Sigman DM, Altabet MA, Michener R, McCorkle DC, Fry B & Holmes RM (1997) Natural abundance-level measurement of the nitrogen isotopic composition of oceanic nitrate: an adaptation of the ammonia diffusion method. *Mar. Chem.* 57: 227–242
- Stream Solute Workshop (1990) Concepts and methods for assessing solute dynamics in stream ecosystems. *J.N. Am. Benthol. Soc.* 9: 95–119
- Suberkropp K & Klug MJ (1976) Changes in the chemical composition of leaves during processing in a woodland stream. *Ecology* 57: 720–727
- Suberkropp K & Chauvet E (1995) Regulation of leaf breakdown by fungi in streams: Influences of water chemistry. *Ecology* 76: 1433–1445
- Tank JL, Meyer JL, Sanzone DM, Mulholland PJ, Webster JR, Peterson BJ, Wollheim WM & Leonard NE (2000) Analysis of nitrogen cycling in a forest stream during autumn using a <sup>15</sup>N tracer addition. *Limnol. Oceanogr.* 45: 11013–11029
- Tank JL & Webster JR (1998) Interactions of substrate and nutrient availability on wood biofilm processes in streams. *Ecology* 79: 151–162

- Vitousek PM, Aber JD, Howarth RW, Likens GE, Matson PA, Schindler DW, Schlesinger WH & Tilman DG (1997) Human alteration of the global nitrogen cycle: Sources and consequences. *Ecol. Applic.* 7: 737–750
- Webster JV & Ehrman TP (1996) Solute dynamics. In: Hauer FR & Lamberti GA (Eds) *Methods in Stream Ecology* (pp 145–160). Academic Press, San Diego
- Welshmeyer NA (1994) Fluorometric analysis of chlorophyll *a* in the presence of chlorophyll *b* and pheopigments. *Limnol. Oceanogr.* 39: 1985–1992
- Wetzel RG & Likens GE (1991) *Limnological Analyses*. Second ed. Springer Verlag
- Winterbourn MJ (1990) Interactions among nutrients, algae, and invertebrates in a New Zealand mountain stream. *Freshw. Biol.* 23: 463–474
- Young RG & Huryn AD (1998) Comment: Improvements to the diurnal upstream-downstream dissolved oxygen change technique for determining whole-stream metabolism in small streams. *Can. J. Fish. Aquat. Sci.* 55: 1784–1785